“Keratins in β-cells of the pancreas and their role for mitochondria and insulin vesicles”

Angeli Kumari-Ilieva

Master’s thesis

Åbo Akademi University

Department of Biosciences

10.3.2019

Master’s degree in Biomedical Imaging Programme

Specialization theme

Supervisors

1. Jonas Silvander MSc and
2. Diana Toivola PhD

ÅBO AKADEMI UNIVERSITY

Department of Biosciences

Faculty of Science and Engineering

ANGELI KUMARI-ILIEVA: Keratins in β-cells of the pancreas and their role for mitochondria and insulin vesicles

Master's thesis

March/2019

Abstract

Keratin intermediate filaments are structural proteins that are involved in protecting the epithelial cell from outside stress. Extensive research has been done on their role in several organs such as the liver. However, very little is known of their roles in the endocrine pancreas, where keratin 8 and 18 (K8/K18) are the main keratins expressed. Published data from Toivola laboratory showed that the mitochondria in β-cell knockout samples appeared to be smaller and fragmented. Therefore, the first aim of this thesis was to analyse, in further detail, the role of keratins in β-cell mitochondrial morphology and function. In order to study keratins in β-cell mitochondria a model was used. This was using keratin wild type and knockout mice to obtain primary β-cells. Therefore, one objective was to obtain another method to study the function of keratins. For this the aim was to transfect K8/K18 into the β-cell MIN6 cell line and establish a stable cell line that could be used for research and that could act as one more model. The final aim was to use the keratin transfected MIN6 cells and to see weather keratin presence had an effect on insulin vesicle amount and vesicle location.
Increased fragmentation of mitochondria in cells lacking keratins was found. This was determined by a blind study which involved analysing various images of 3D projection of mitochondria and categorizing them according to their fragmentation. Next the mechanism behind the fragmentation was explored using western blotting analysis. This revealed decreased levels of proteins such as MFN2 and Tchp in knockout mice which are thought to be involved in linking the keratins to mitochondria.
Unfortunately, transfecting fluorescent keratins into MIN6 cell by using various different transfection methods proved to be ineffective with a maximum transfection efficiency of 10%. Finally, transfected and stained MIN6 cells, showed that MIN6 cells with keratins contained more insulin vesicles than MIN6 cells without keratins.

Key words: Keratin - Mitochondria - Beta cells - MIN6 - Islets - Keratin 8-null mice - Fusion-Transfection- Insulin

List of abbreviations

GSIS	Glucose stimulated insulin secretion
IF	Intermediate filament
K	Keratin
$K8^{+/+}$	Keratin 8 wild type
$K8^{-/-}$	Keratin 8 knock out
MFN	Mitofusin
MIN6	Murine insulinoma cells
OPA1	Optic atrophy type 1
OXPHOS	Oxidative phosphorylation
TCHP	Trichoplein
TEM	Transmission electron microscope
TOM	Translocase of outer membrane

TABLE OF CONTENTS

1. LITERATURE REVIEW

1.1 The Cytoskeleton

1.1.1 Constituents of the cytoskeleton: Microfilaments, Microtubules, Intermediate filaments

The cytoskeleton is a collective term for structural fibres that are crucial parts of a cell. It can be described as a dynamic structure, since it is made of units that can be rapidly removed or added when needed (Bragulla and Homberger 2009). The cytoskeleton is made up of three main units of different sizes and function which will be discussed in further detail below.

Microfilaments are the smallest of all three cytoskeletal units. They are 7 nanometre (nm) in diameter and are also referred to as actin filaments since they are entirely made from actin which is involved in e.g. muscle contraction. Actin filaments are polarized as they have a negative end and a positive end which contribute to their function in muscle contraction (Bragulla and Homberger 2009). Apart from being part of muscle contraction, actin plays an important role in a variety of cellular processes, such as cell motility and cell division (Alberts et al., 2002).

The next cytoskeletal subunits in size are the intermediate filaments (IF); these are on average 10 nm in diameter (Cooper and Sunderland 2000; Lowery et al., 2015), and can vary between 7 and 12 nm in diameter (Bragulla and Homberger 2009). IFs can be further divided into six different classes, type I and II being keratins, type III containing vimentin, desmin and peripherin, type IV such as neurofilaments, V nuclear lamins and lastly type VI nestin (Cooper and Sunderland 2000). Unlike the microfilaments, IFs are composed of several different types of proteins and do not have positive and negative ends. In the human body, these IFs can be found in a variety of locations (see table 1). Type I and II (keratins) are expressed in epithelial cells. Type III can be found in a variety of cells ranging from fibroblasts to white blood cells. Type IV is found in neurons, whereas type V in the nuclear lamina and type VI in stem cells.

Although found in a variety of sizes and in different location, IFs share important structural similarities. IFs have a structurally conserved central rod domain. This central

rod domain is α-helical and its subdomains are connected by linker domains (Bragulla and Homberger 2009). In addition, IFs also consist of globular head and tail domains whose N- and C-terminals show more diversity than the rod domains by varying in size and sequence between different IFs (Williams et al. 2015 & Coulombe et al., 2001).

Table 1. Intermediate filament protein types and their site of expression (Cooper and Sunderland 2000).

Type	Protein	Size (kd)	Site of expression
I	Acidic keratins	40–60	Epithelial cells
	(~15 proteins)		
II	Neutral or basic keratins	50–70	Epithelial cells
	(~15 proteins)		
III	Vimentin	54	Fibroblasts, white blood cells, and other cell types
	Desmin	53	Muscle cells
	Glial fibrillary acidic protein	51	Glial cells
	Peripherin	57	Peripheral neurons
IV	Neurofilament proteins		
	NF-L	67	Neurons
	NF-M	150	Neurons
	NF-H	200	Neurons
	α-Internexin	66	Neurons
V	Nuclear lamins	60–75	Nuclear lamina of all cell types
VI	Nestin	200	Stem cells of central nervous system

Microtubules are the largest of the three IFs, with a diameter of 25 nm (Mikhailova et al., 2016). They are made from two subunits, alpha and beta tubulin, which together make microtubule fibres used in e.g. flagella and cilia. Unlike the other cytoskeletal proteins, microtubules make a hollow tube which also gives rise to their name.

1.1.2 Keratins

Keratin IFs are structural proteins that are found in epithelial cells (Hermann and Bragulla 2009). From the IFs subtypes I-V, I and II are keratins. Type I are classified as acidic keratins and type II are basic keratins. Most notably keratins are known to protect the cell from outside stress (Toivola et al., 2010). Like other IFs, they are structurally made from a highly conserved central coil-coil α-helical rod domain and a non α-helical head and tail domain (Omary et al., 2009). It should be noted that the IFs are assorted into their respective groups according to the highly conserved amino- acid sequence of the rod

domain. Interestingly, unlike the other IFs, keratins are formed as heteropolymers meaning that they can only exist if there is one of each, type I and type II keratin (Hermann and Bragulla 2009).

Collectively, type I and type II keratins have a molecular weight (MW) ranging from 40 to 70 kDa (Sun et al. 1983; book Cooper and Sunderland 2000) and more specifically for acidic type I keratins the MW ranges from 40 to 60 kDa and for type II it varies between 50 and 70 kDa. There are other subtle differences between the two different types of keratins. For instance, type II keratin´s head domain consists of three subdomains: end domain (E1), variable domain (V1) and a homologous domain (H1) (as seen in Fig 1). Contrary to this, the head domain of type I keratins does not contain a homologous subdomain (H), and. thus consists of only V1 and E1 subdomains (Bragulla and Homberger 2009). The same applies to the tail domains of keratin filaments where type II keratin tail domain consist of three subdomains (H2, V2 and E2) and type I consists of only V2 and E2 (Bragulla and Homberger 2009; Steinert et al., 1985).

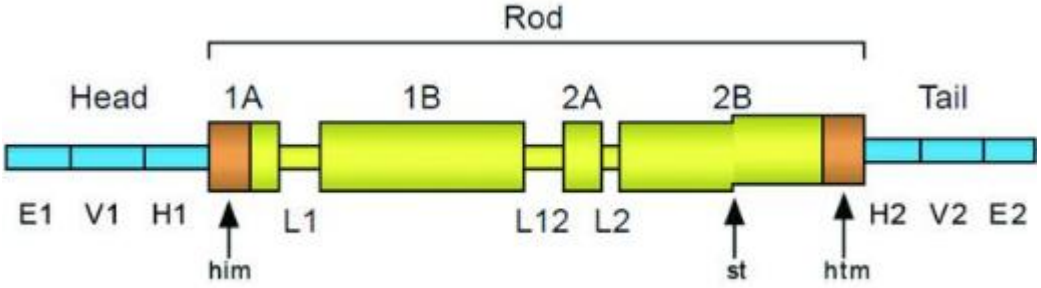

Figure 1. Secondary structure of keratin type II protein containing head, rod and tail domains (Bragulla and Homberger 2009). Keratin type I protein would otherwise be the same, except the head domains would only consist of variable (V) and end (E) domains.

Keratin filaments are formed when two monomers first form a coiled-coil dimer, these dimers then in turn line up (in opposite directions) to create tetramers. Two tetramers can then associate to one repeatedly, until creating the quaternary structure of a keratin filament (Bragulla and Homberger 2009).

There are 37 genes that code for epithelial keratins and from these type I is coded by 19 genes and type II by 17 genes (Omary et al. 2009). The main keratins found in the endocrine pancreas are K8 and K18, and to some degree K7 is also present in mice (Alam et al., 2013).

K8 and K18 are the keratins that this project will be looking further into. K8 (Basic keratin, soft, type II) has a MW of 52.2 kDa and isoelectric pH of 6.1 (Moll et al., 1982). It forms a heterodimer in a manner explained above with K18 (soft, type I) MW of 44 kDa and an isoelectic pH of 5.5 (Hutton et al., 1998).

1.1.3 Keratin functions, mutations and disease

Keratins have several functions in cells and one of the most important functions of keratins is to provide cells with mechanical stress support (Toivola et al., 2010). This cytoprotective role is highlighted by studies like Asghar et al., 2015 where reduced amount of keratins during induced colitis is linked to lack of colon protection. Furthermore, keratins are upregulated during stress situations (both in humans and in mice) which reinforces the important function of keratins as stress protectors (Helenius et al., 2016; Zhong et al., 2004). Apart from functioning as cellular stress proteins (Toivola et al., 2010), keratins have many other functions. For instance, they have been shown to regulate mitochondrial morphology in hepatocytes (Tao et al., 2009) as well as in the endocrine pancreas (Alam et al., 2013).

IFs can be found in a vast variety of cells in the human body (see table 1) and subsequently abnormalities of IFs affect numerous organs. Over 80 human diseases are caused or predisposed by genetic mutations of IFs (Omary et al. 2009). For instance, keratin mutations (keratinopathies) have been shown to cause several skin disorders (Chamchau et al., 2010) and predispose to liver diseases (Toivola et al., 2015), whereas mutations in lamins (laminopathies), such the mutation in lamin A, have been shown to be the cause of Hutchinson-Gilford progeria syndrome (Hennekam 2006). HGPS, first described by Jonathan Hutchinson in 1886, is an extremely rare (1 in 4 million births) (Hennekam 2006) and debilitating disease that mimics the human aging process; however, the aging begins in childhood and rapidly progresses.

Simple epithelia can be found in numerous tissues and organs and, thus, it is not surprising that simple epithelial keratin mutations are potentially involved in diseases affecting several organs of the human body. Depending on the type of tissue that is in question, different types of keratins are expressed and thus different types of keratins are involved in potential keratin pathologies. For instance, K8 and K18 are predominantly found in the liver, digestive organs and the pancreas (Omary et al., 2009; Toivola et al., 2015) and thus these keratins are the main keratins that are associated with liver diseases.

1.1.4 Simple epithelial keratins and the endocrine pancreas

The specific roles of keratins in the pancreas is still largely not known; however, it has been shown that K8 and K18 are the main keratins in the endocrine pancreatic islets with remnant K7 (Alam et al., 2013; Bouwens 1998). Keratins in other organs appear to play an important part in stress protection exemplified by a study, done by Zhong et al., 2004, where organ-specific stress was shown to induce keratin over expression in mouse pancreas by threefold. Interestingly, however, under generalized stress conditions (heat and water immersions) pancreatic keratin levels were not altered.

From knockout mouse studies it has been suggested that keratins have multiple different functions in the endocrine pancreas. It has been shown (Alam et al., 2013) that in the absence of K8 in β-cells, insulin vesicle morphology changes and appears smaller and irregular. Furthermore, lack of K8 results in the mislocalization of GLUT2 transporter (a transmembrane carrier protein enabling the import of glucose). In addition, the lack of K8 in β-cell mitochondria leads to an increased number of mitochondria appearing fractionated, with an increase of round mitochondria shape over long and oval shapes (Alam et al., 2013). This suggests the potential role of keratins in the fusion of mitochondria. Moreover, the mitochondrial cristae appear to be spread out (scattered) in K8 knockout mice, further emphasizing the role of keratins in the endocrine pancreas (Alam et al., 2013). Furthermore, this study showed that the absence of K8 lead to a reduction in blood glucose levels and resistance to hyperglycaemia, all which indicated the role of keratins in regulating blood glucose levels (Alam et al., 2013).

1.2 The pancreas

1.2.1 The role of the pancreas

In humans, the pancreas is on average a 15-cm long organ (Treuting et al., 2011). Located at the back of the upper abdomen, sitting in the retroperitoneum, it hugs the upper part of the small intestine, the duodenum. It can be described as having three main different regions (Ross and Pawlina 2011), the head (next to the duodenum), the body and the tail. The pancreas is an important gland that is part of the digestive system consisting of two structurally and functionally different parts, the exocrine pancreas and the endocrine

pancreas (Ross and Pawlina, 2011). Most of the pancreas consists of exocrine tissue. In humans the portion of endocrine tissue is about 1-2% (Treuting et al., 2011). The exocrine pancreas plays an important role in producing digestive enzymes, such as amylase, which breaks down carbohydrates into glucose, protease, which breaks down proteins into amino acids and lipase, which break down lipids.

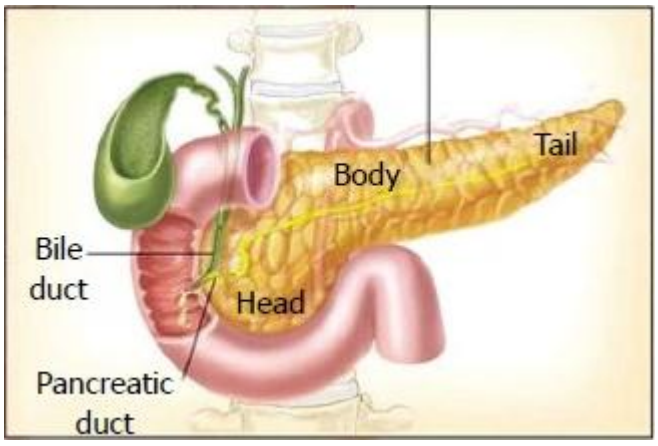

Figure 2. Anatomy of the pancreas, showing the location of the bile duct and pancreatic duct (Cid-Arregui and Juarez 2015).

1.2.2 Endocrine pancreas

The endocrine tissue of the pancreas consists of the islets of Langerhans, so called after the German anatomical pathologist who discovered them in 1869 (Gaw 2008). These islets contain mainly three different cell types, α, β and δ-cells (Gaw 2008). The α-cells secrete glucagon which increases glucose concentration by releasing it from storage, whereas β-cells secrete insulin which in turn stimulates the storage of glucose. β-cells also secrete amylin, which slows down the gastric emptying. It should be noted here that most of the human endocrine pancreas consists of β-cells, whereas the second most numerous cells are the α-cells (Treuting et al., 2011). δ-cells are the least numerous, contributing to only about 10% of the endocrine tissue (Elayat, el-Naggar, Tahir 1995). δ-cells secrete the hormone somatostatin, which among its many functions inhibits the secretions of the hormones glucagon and insulin. Finally, present in the islets are also other cells but in much lower numbers. These are the Ɛ-cells and PP or F cells, the former producing ghrelin and the latter secreting pancreatic polypeptides (Treuting et al., 2011).

1.2.3 Endocrine pancreas and glucose uptake

The release of insulin from the β-cells of the endocrine pancreas is glucose depended

(Llanos et al., 2015). With the rise of blood glucose levels, insulin hormone is released and produced by the cells. Most crucially, insulin stimulates the uptake of glucose by target tissues.

Initially glucose is taken up by β-cells by facilitated diffusion through glucose transporters GLUT2 (Komatsu et al., 2013). This leads to elevated glucose levels within the cell. Once glucose enters the cells it undergoes glycolysis, followed by the Krebs cycle and oxidative phosphorylation. The latter produces ATP's leading to increased levels of ATP within the cell. This is turn causes the potassium (K+) channels of the cell to close. As a result, causing a depolarization of the cell which stimulates the voltage gated Ca^{2+} channels leading to an influx of Ca^{2+} into the cell. Finally, the increased levels of Ca^{2+} stimulate the release of insulin vesicle by exocytosis leading to the release of insulin into the blood stream (Llanos et al., 2015).

1.2.4 Diabetes Mellitus

The pancreas is the main organ involved in the development of diabetes mellitus. There are two main types of diabetes mellitus. Insulin dependent (also known as type 1) and non-insulin dependent (also known as type 2). Both are metabolic disorders that involve the inability to regulate glucose levels, but pathologically they are very different (Gaw et al., 2008). Type 1 diabetes can affect anyone at any point of age, but in general has a much earlier onset than type 2 (Diaz et al., 2015) and it involves autoantibodies that attack the insulin producing β-cells. In its essence, it is an autoimmune destruction of the insulin producing tissue. On the other hand, type 2 diabetes has had a much later onset (in adulthood), however epidemiological data increasingly shows the incidences in children to be on the rise (Mayer-Davis et al., 2017). Type 2 diabetes, unlike type 1 diabetes, is not an auto-immune disorder, instead it results from insulin resistance that develops over a long period of time. In type 2 diabetes the β-cells can produce insulin, however, the muscle cells are resistant to it (Kahn et al., 2014).

1.3 Mitochondria

1.3.1 Structure and function

The mitochondrion is a fascinating organelle, containing its own mitochondrial DNA, which is inherited from the mother solely (Giles et al., 1980). Humans have two genomes, the nuclear genome and mitochondrial genome. Due to having its own DNA, it is thought to have originated as an organism on its own which was engulfed by an eukaryotic cell (Wilson and Hunt, 2008; Gray et al., 1999).

The mitochondrion (plural mitochondria) consists of two membranes (outer and inner membrane) made up of a phospholipid bilayer (see figure 3, shows an illustration of a mitochondria) (Blanco et al.,2011). The outer membrane contains porins, which do not allow large molecules to pass passively. Only small molecules, like ions and pyruvate, can pass through porins. The inner membrane consists of numerous folds referred to as crista (plural cristae) (Frey and Mannella, 2000). These increase the surface area available for ATP production (oxidative phosphorylation). The area between the outer and inner membranes is called intermembrane space, whereas the area inside the inner membrane is called the matrix, where the Krebs cycle occurs.

As the Krebs cycle (citric acid cycle) and oxidative phosphorylation take place in mitochondria, they are often described as the energy factory of the cell. The Krebs cycle takes place in the matrix of the mitochondria where pyruvate enters into the mitochondria and is converted into acetyl-CoA which then enters the Krebs cycle. A series of reactions follow resulting in the production of two molecules, $NADH_2$ and FADH (Berg et el., 2002; Jitrapakdee et al., 2010). These molecules then enter the final step of cellular respiration called oxidative phosphorylation, which takes place on the inner membrane, which is embedded with enzymes constituting the electron transport chain. There are five main enzymes involved in oxidative phosphorylation: I NADH reductase, II Succinate dehydrogenase, III Cytochrome reductase, IV Cytochrome oxidase and V ATP synthase. The passing of electrons (passing from higher energy to lower energy states) results in energy production, which in turn results in hydrogen ions (H^+) being pumped into the intermembrane space. Finally, these hydrogen ions will be transported back into the matrix by the last enzyme ATP synthase. This final step results in ATP production.

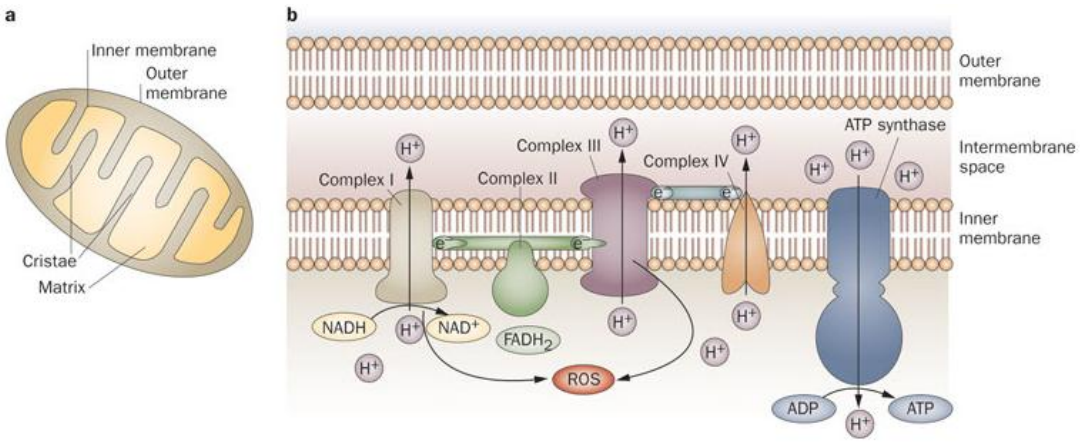

Figure 3. The structure of Mitochondria. a: Structure of Mitochondria b: Phospholipid bilayer and proteins involved in the electron transport chain. (Blanco et al., 2011)

1.3.2 Mitochondria and keratins

No research had been done prior to this study on the relationship between β-cell mitochondria and keratins in the pancreas, however, studies have been done in hepatocytes and surface epithelia which linked keratins to mitochondrial function (Tao et al., 2009; Kumar et al., 2015). For instance, Tao et al., 2009 compared mouse liver protein expression profiles from K8 wild type mice to those of K8 knock out mice, and the results showed that livers that lacked K8 (or had disrupted K8) have altered protein expression profiles. These findings highlight the involvement of keratins in mitochondrial health and function. In addition, Alvaro and Coulombe (2014) studied the effect of keratins in skin and their results showed that a deletion of Krt5 in mice resulted in a major decrease in the percentage of normal mitochondria in Krt5 null mice, further emphasising the involvement of keratins in mitochondrial function. A similar link between keratins and mitochondria in skin had previously been mentioned by Takahashi et al., in 1994.

1.3.3 Mitochondrial fission and fusion

Mitochondria are dynamic organelles which undergo fission and fusion. These processes are crucial for the health of the mitochondria, as by these two mechanisms the mitochondria can respond to changing environments, such as increased stress or decrease in nutrients and, most importantly, avoid genetic malfunction (Hales and Karen 2010). In a low-stress environment, the mitochondria fuse (Liesa and Shirihai 2013) which also allows for content mixing, whereas during high stress or apoptosis the mitochondria undergo fragmentation (Molina et al., 2009). These crucial processes, by which the

mitochondria respond to their surroundings, are regulated by the cytoskeleton and other related proteins, and the mechanism by which these processes occur will be discussed below (Molina et al., 2009; Woods et al., 2016; Hatch et al., 2014).

Mitochondrial fusion is a two-step process (Liesa et al., 2009) in which the inner and outer membranes fuse separately (Malka et al., 2005). This involves several GTPases: Mitofusin 1 (MFN 1), Mitofusin 2 (MFN2) and Optical atrophy 1 (OPA1) (Hales and Karen 2010). MFN1 and MFN2 are located both on the outer mitochondrial membrane, whereas OPA1 is located in the inner membrane (Liesa and Shirihai 2013). Respectively, Mitofusins aid in the fusion of the outer membrane, where as OPA1 leads the fusion of the inner mitochondrial membrane (Liesa et al., 2009). The importance of these proteins is highlighted by the diseases they are associated with, such as Charcot-Marie Tooth (a group of hereditary neuropathies) type 2A, which is caused by a mutation in MFN2(Liesa et al., 2009).

In the case of fission, another protein (DRP1) belonging to the GTPase is in charge. Dynamin related protein (Drp1) mediates the fission of mitochondria by binding to OMM proteins (for example Fis1), which leads to a constriction (see figure 4 b) and subsequently, fission is completed (Liesa and Shirihai 2013).

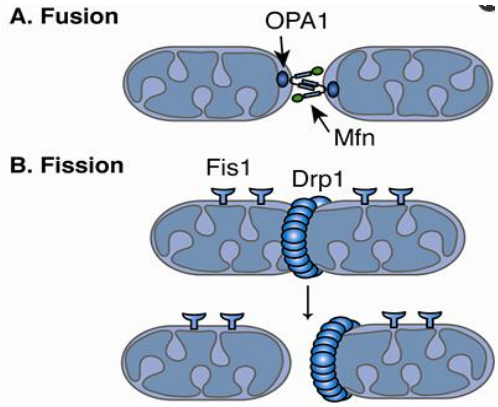

Figure 4. Illustration of a mitochondrial fusion process where OPA1, Drp1 and MFN (Mfn) are proteins involved in the fusion and fission processes. a) mitochondria fusion and b) mitochondrial fission (Chen and Chan 2006).

1.4 Insulin vesicles

1.4.1 Insulin structure and synthesis

Insulin is a relatively small protein of about 6 kDa (Weiss et al., 2000) and consists of 51 amino acids (Fu et al., 2013). It is made from two chains (A and B) that are held together by disulphide bonds (Fu et al., 2013). Most importantly, the amino acid sequence of insulin in mammals is highly conserved, which allows for insulin that is produced in a pigs pancreas to be used by humans. Insulin is secreted in response to elevated glucose levels. The process is described as biphasics (Jitrapakdee et al., 2010) as it occurs in two phases. Initially, preformed insulin, located in an insulin vesicle near to the cell membrane, is secreted from β-cells, leading to an initial spike of insulin in the blood (see figure 5 below). As this is occurring, the cell begins to produce more insulin to meet the demand. This leads to the second, slower, insulin release phase (Olofsson et al., 2002). Insulin is synthesised as pre- pro insulin in ribosomes of the rER. This is then cleaved to pro-insulin and transported to the Golgi apparatus (Fu et al., 2013).

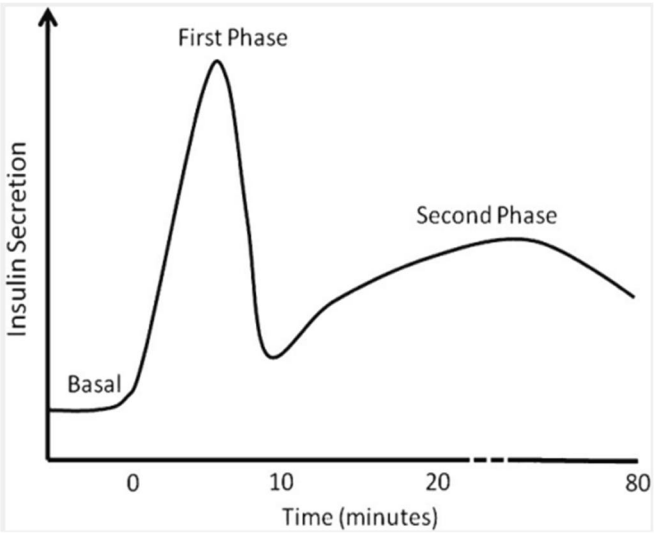

Figure 5. Insulin secretion. Initial large increase of insulin secretion that is seen in the first phase is from stored insulin in the cell. However, once it's used up the levels fall while new insulin is formed (Meloni et al., 2012).

1.4.2 Molecular mechanisms behind glucose dependent insulin release

Initially glucose is taken up the β-cells by facilitated diffusion through glucose transporters GLUT2 (figure 6) (Jitrapakdee et al., 2015). This leads to elevated glucose levels within the cell. Once glucose enters the cells it undergoes glycolysis, followed by the Krebs cycle and oxidative phosphorylation. The latter produces ATP's, leading to increased levels of ATP within the cell. This in turn causes the potassium (K+) channels of the cell to close. As a result, causing a depolarization of the cell which stimulates the voltage gated Ca^{2+} channels, leading to an influx of Ca^{2+} into the cell. Finally, the increased levels of Ca^{2+} stimulate the release of insulin vesicles by exocytosis, leading to the release of insulin into the bloodstream (Hao et al., 2005).

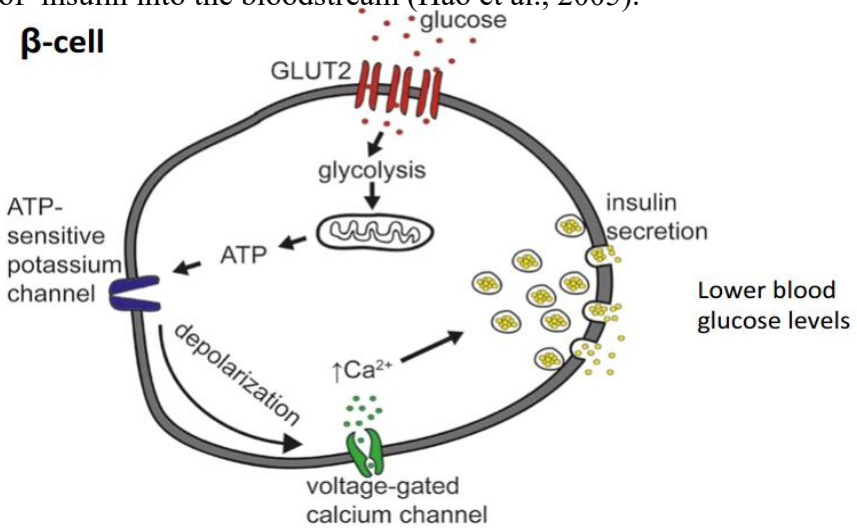

Figure 6. Schematic representation of GSIS (Silvander 2018).

1.4.3 Transfection

Transfection is a method by which foreign genetic material (nucleic acids) is introduced into eukaryotic cells. Transfection can be divided into two different types based on the amount of time that the foreign nucleic acids are present, transient and stable (Kim and Eberwine 2010). In transient transfection, the newly introduced genes are expressed temporarily. On the other hand, in stable transfection the new genetic material is incorporated into the host genome and thus is expressed permanently.

There are different ways of introducing foreign genetic material into a eukaryotic cell (Kim and Eberwine 2010). Depending on the cell line, one can choose e.g. reagent based, instrument based or by using a viral vector. In reagent based methods, such as lipid based techniques, the foreign nucleic acids associate with the lipid compound, coating the nucleic acids. The lipid-DNA complex can then fuse or be endocytosed by the host cell

allowing for the foreign DNA to be introduced to the host cell. On the other hand, electroporation is a method by which foreign genetic material is introduced into the target cell by fragmenting the cell membrane. This is done by applying an electric field which permeabilizes the cell membrane, allowing for the plasmids to enter the target cell.

2. AIMS AND HYPOTHESIS

2.1 Aims

In order to study the role of keratins in *β*-cell mitochondrial regulation, insulin vesicle amount and localisation, this master's thesis will be formulated into three different aims:

1) Investigate the role of keratins in pancreatic *β*-cell mitochondrial fusion and fission

2) Determine the best method for transfecting K8/K18 into MIN6 cells;

3) Investigate the amount of insulin vesicles in K8/K18 positive MIN6 cells, and study the location of insulin vesicles in MIN6 cells.

2.2 Hypothesis

Keratins are important for normal mitochondrial homeostasis, insulin vesicle amount and localization in β-cells.

3. MATERIALS AND METHODS

3.1 Animal models

Keratin positive ($K8^{+/+}$) mice cells and keratin negative, i.e. knock out ($K8^{-/-}$), mice cells (FVB/n background) were used in the experiments (Baribault et al., 1994). All animal experiments were approved by the National Animal Experiment Board and conformed to the regulations set by the Finnish Act on Animal experimentation.

Sacrificing mice and islet isolation

Mice are sacrificed by asphyxiation (with CO_2), after which an incision is made in the abdomen. The abdomen is cut open in order to have access to the pancreas. Islet isolation is done by following the protocol outlined by Alam et al., 2013. The only step that differs from the ones outlined by Alam et al., 2013 is the first step, where the pancreas is first placed into a 50 ml tube on ice and then collagenase solution (Collagenase P (Roche, Mannheim, Germany) in Hanks Balanced Salt Solution (Sigma-Aldrich)) is injected through the common bile duct. The collagenase is added in order to bloat the pancreas and to digest it. From this point forward the protocol is identical to that outlined by Alam et al., 2013, with the main steps summarised here shortly. After the pancreas is placed into the falcon tube with the collagenase solution and HBSS is added, the pancreas is then incubated for 16 min at +37ºC, in order to digest it. After this, the pancreas is placed on ice with 15 ml RPMI-medium in order to stop the digestion. The tube is then vortexed to break the tissue apart, and most importantly, to separate the islets from the exocrine tissue. This step is followed by a "layering step", where the aim is to separate layers of liquid by gradient centrifugation, where the islets will be in the middle layer. This layering of liquids is achieved by adding two different liquids with different densities. These liquids are 10 ml of Histopaque 1077 (Sigma-Aldrich) and 10ml HBSS. This allows for the islets to migrate to the interphase between the Histopaque and HBSS and, thus, separating from the exocrine cells. The islets are then picked and transferred into another 50ml falcon tube. Finally, several washing steps follow which aim at removing the leftover Histopaque 1077 (Sigma-Aldrich) and HBSS. Following this, the islets are placed in RPMI and serum on a cell culture dish. After the islets of Langerhans have been separated from the rest of the pancreas, they are stored aside for later use. The type of mice to be used are $K8^{+/}$ and $K8^{-}$

/-.

3.2 Cell culture, transfection and fixation

Murine insulinoma (MIN6) (mycoplasma-free, Adex Bio,San Diego,CA,USA) cells are used. The cells are kept in cell flasks (25m^3, Sarsted, Numbrecht, Germany) and grown in DMEM (Dulbecco's Modified Eagle's Medium), which has (15%) Foetal calf serum added to it, in addition to (14.5%) β-mercapto ethanol (Sigma-Aldrich), sodium pyruvate, 1% penicillin and GlutaMax (see appendix 8.2). The cell passages used are from 20-45 passages; this is because after passage 60, these cells stop producing insulin (Cheng et al., 2012). Cells are to be grown until 70-80% confluence and then split. This is done about once a week. In addition, 3-4 days after splitting the cells media are changed in order to provide new nutrients and to flush out any dead, unattached cells.

Transfection

Two different transfection methods were used to transfect non-fluorescently labelled K8 (keratin 8) and K18 (keratin 18) into the MIN6 cells. The methods chosen are electroporation and Lipofectamine 3000. The confluence of the cells, prior to transfection, will vary according to the requirements of the transfection method. For electroporation, the confluence will be about 50%, whereas for Lipofectamine 3000 required confluence is 70-80%.

Electroporation

A flask of MIN6 cells is washed three times with PBS, after which trypsin is added for 5 min at 37ºC, to detach the cells from the bottom of the flask. Following this, the cells are transferred into a falcon tube, and 15ml DMEM media (see appendix 8.2) is added. The cells are centrifuged for 5 min at 800rpm, after which the supernatant is removed and the pellet is resuspended in 400 µl Optimem (Invitrogen, CA, USA). Keratin 8/18 plasmids (10 µg, Addgene, Cambridge, MA, USA) are then added into a cuvette , followed by adding the MIN6 cell-Optimem mixture into the cuvette. The cuvette is then electroporated using a gene pulser (Bio-Rad, CA, USA), with settings at 220V and 975 µF. Electroporated cells are then removed from the cuvette and added into a falcon tube, with 20ml media. This media is then pipetted onto a 24 well plate (0.5-1 ml per well) with

coverslips at the bottom.

Lipofectamine 3000

Transfection with Lipofectamine 3000 (Thermofisher) is done by following the protocol provided by Thermofisher. Notably, unlike electroporation, this method requires a higher confluency (70%). See appendix 8.3 for example of experimental protocol. Transfection was done in 6-well plates.

Each well will contain:
1.5 µl* Lipofectamine 3000 reagent 25 µl Optimem 2 µl P3000 reagent 5 µg K8 (non-fluorescent) 5 µg K18 (non-fluorescent)

*Note that this same protocol was repeated with Lipofectamine 3000 concertations 3.7 µl and 7.5 µl.

Protocol:

1. Change media* of cells (each well=500 µl media)
2. In a 50 ml eppendorf tube add:
    - 250 µl Optimem
    - 14 µl Lipofectamine
3. In another 50ml eppendorf tube add:
    - 250 µl Optimem
    - 7 µl K8 and 10µl K18
    - 10 µl P3000 reagent
4. Mix solutions from 2 and 3 and incubate for 5 min in room temperature.
5. Add the solution to 24 well plates. 25 µl per well.

*Recipe for MIN6 Media:

600 ml DMEM (Dulbecco's Modified Eagle's Medium)

6 ml 15% Foetal calf serum (Biowest)

6 ml sodium pyruvate,

6 ml 1% penicillin (Gibco)

6 ml GlutaMax

14.5% β-mercapto ethanol

Fixation

MIN6 cells that are stained for immunofluorescence are seeded onto a 6 well or 24 well plates with glass added to the bottom, and after 2 days they are washed with PBS, fixed with 1% PFA (Sigma-Aldrich) for 20min at room temperature and stored in +4ºC.

3.3 SDS-PAGE and western blotting

Blotting in molecular biology refers to the process of transferring DNA, RNA or proteins onto a membrane (webster dictionary). The 4 main methods used are: southern blotting (detection of DNA), northern blotting (detection of RNA), eastern blotting (detection of post-translational proteins) and western blotting (detection of proteins).

SDS-Page

Running proteins through a gel is the first step in the western blotting protocol. The aim of running an SDS-page (sodiumdodectyl sulfate polyacrylamide gel electrophoresis) is to separate the proteins in a given sample (Albert and Lewis 2002). Polyacrylamide gel is used as a medium through which the proteins move. This is because it is a porous material, allowing for undisturbed movement of the proteins through the gel and it is also biochemically inactive, meaning that the proteins will not interact with the gel. Note that the size of the pores can be varied by varying the acrylamide concertation of the gel. The proteins of interest, in our case, range from 14 to 86 kDA. Therefore, the acrylamide concentration used will vary between 10-12%. The lighter the protein of interest, the higher the acrylamide concentration of the gel. The gel consists of two parts, the stacking gel (pH 6.8) on the top containing wells into which the specimen is loaded, as well as, a bottom gel called the resolving gel (pH 8.8). SDS not only denatures the proteins, but it also binds to the proteins and gives them a net negative charge, ensuring a unidirectional movement of all proteins in one direction, from the negative end (cathode) towards the positive end (anode), once the electric field is applied. The smaller the protein,

the faster it moves through the gel as it will experience less resistance, allowing the sample mixture of proteins to be spread out over the surface of the gel according to their size (measured in kilo Daltons, kDa). In addition, the sample will contain a dye, such as bromophenol blue. Due to the small size of the dye molecule, it will move across the gel fastest, ahead of the proteins, and is used as an indication to stop the running of the gel when the dye front reaches near the bottom of the gel. In this case, the average running time is about 90min at 120V.

SDS-page gels will be made with varying acrylamide concentration ranging from 10-12%, depending on the size of the protein of interest. Following this, the samples will be run and transferred onto a PVDF membrane.

Western blotting

Western blotting (Burnett 1981), also sometimes referred to as immune blotting, is a highly sensitive technique that utilises antigen and antibody interactions. It is widely used as a mean to verify the expression of a protein (or lack thereof) in a sample. In addition, it allows for the quantification of the amount of protein in a given sample. This allows for the comparison of the amount of protein between different samples. After running the samples on the SDS-page, the separated proteins will be transferred onto a PVDF (polyvinylidene difluoride) membrane. To facilitate the migration of the proteins, form the gel onto the PVDF membrane, a "sandwich" containing the gel at the bottom and the PVDF membrane on top of it, is made. This was done by stacking a sponge at the bottom, on top of it two filter papers followed by a gel and a membrane on top of it and finally another set of filter papers were added with a sponge at the very top. The whole sandwich is held together by a cassette, which was immersed in a tank containing transfer buffer (see appendix for recipe). An electric field is applied of 100V for 60 min at 4ºC. Once the transfer was complete, the membrane is either left to dry, or used right away. It must be noted that, dry PVDF membranes must always be activated in methanol before use.

The first step of blotting is blocking with an unspecific protein, which aims to increase sensitivity by preventing non-specific binding of the primary antibody, which is added later. In this case, blocking was done by adding a solution of 5% milk in PBS-Tween onto the membrane for 60 min. The blocking agent here is the milk protein casein. After this, the membrane is washed three times for 5 min with a solution of PBS-Tween. Following this a primary antibody (table 1.) specific for the protein of interest is added for 60 min at

room temperature or overnight at 4ºC. Another washing step followed, washing three times with PBS- Tween, as before, the membrane is incubated once more with a secondary HRP conjugated antibody for 60 min. Once again, a washing step followed, as before and finally the membrane was incubated for 60 seconds with a chemiluminescent substrate ECL (GE Healthcare) (enhanced chemiluminescence), which reacts with the enzyme HRP of the secondary antibody producing light that can be detected by using light sensitive x-ray films (Fuji, Tokyo, Japan). The membrane and the light sensitive film was added into an exposure cassette, and the films were developed with varying developing times in a dark room. The films are then scanned and the blots quantified with ImageJ (National Institute of Health, Bethesda, MD, USA) and the results plotted on graphs using GraphpadPrism 5 (GraphPad, Software, La Jolle, Ca, USA).

Table 2. Proteins of interest that were blotted for

Antibody	Manufacturer	MW (kDa)	Host	Gel %
K8 (troma1)	HDB	54	Rat	10
MFN2	Sigma	86	Rabbit	10
Hsc70	Stressgen	70	Rat	10
COX IV	Cell signalling	17	Rabbit	10
TCHP	Santa cruz	61	Goat	10
Cytochrome c	Cell signalling	14	Rabbit	12
Caspase 7	Cell signalling	20	Rabbit	12
B-actin	Novus Bio.	40	Rabbit	10
OPA 1	Cell signalling	90	Rabbit	10

3.4 Immuno-fluorescent staining

Fluorophore is a molecule that can absorb and emit fluorescent light and fluorescence refers to the process by which light is emitted at a lower wavelength than the light (electromagnetic radiation) that was absorbed. Fluorescent microscopy utilizes the emitted light as a way for visualizing structures, or processes within cells. Immunofluorescence is based on this phenomenon. More specifically, immunofluorescence uses antibodies to stain proteins. It is a type of immunostaining that utilises the antibody-antigen relationship which is very specific and as such, a fluorophore can be bound to an antibody, which then in turn will specifically bind to its antigen.

(Lakowicz 1999; Sovboda and Yasuhida 2006). The resulting slides can then be imaged using e.g. a fluorescent microscope or a spinning disk microscope.

Staining transfected MIN6 cells for keratins, nuclei and insulin vesicles

MIN6 cells, transfected with K8 and K18 and fixed with 1% PFA are fluorescently stained for keratins, nuclei and insulin vesicles. In order to allow for the dye to enter the cells, the cells need to be first permeabilized. This was done with NP-40 (Applichem), after which the slides were washed three times with PBS-Tween (Sigma-Aldrich). In order to prevent non-specific binding, the cells were blocked with buffer A (2.5% BSA in PBS) for 5min and with buffer C (for recipe see appendix). After this, the cells were incubated with the antibodies of interest. For the insulin stain, different primary antibodies (see table 2) were tried in order to see if a better quality image could be obtained. In addition, different incubation times were tested, either 1 hour at room temperature or overnight at 4ºC. Another washing step is performed with PBS, after which, a secondary antibody is added and is incubated for 1 hour at room temperature. The secondary antibody is conjugated to a fluorophore, which can emit light at a specific wavelength. After this, the slides are washed three times with PBS, and a nuclear marker Draq5 is diluted in PBS and added onto the slides for 5min. Finally, the slides were mounted with Prolong Gold Antifade (Invitrogen) and were left to dry in the dark overnight.

Staining with mitochondrial membrane marker TOM20 in order to study fragmentation

Isolated primary β-cells from sacrificed ($K8^{+/+}$ and $K8^{-/-}$) mice are fixed and fluorescently stained with mitochondrial membrane marker TOM20, as described by Silvander et al., 2017. In summary, the cells are permeabilized with NP-40 (Applichem), following which a primary antibody will be added, which will bind specifically to the membrane proteins in the mitochondria. After incubating with the primary antibody, a fluorescently tagged secondary antibody will be added. Finally, DAPI or DRAQ 5 will be added which will stain the nuclei, and the cells will be mounted on cover slips. The slides are then left to dry overnight.

Table 3. List of primary antibodies

Antibody	Host	Staining concentration	Manufacturer
K8 (Troma I)	Rat	1:1500	Developmental Studies Hybridoma Bank
Insulin	Goat	1:200	Santa Cruz
Insulin	Rabbit	1:200	Santa Cruz
Insulin	Rabbit(new)	1:800	Cell signalling
ATPase	Mouse	1:200	Santa Cruz
TOM20	Rabbit	1:500	Santa Cruz

Table 4. List of secondary antibodies

Antibody	Host	Staining concentration	Manufacturer
Alexa Fluor (488)	anti-Rabbit	1:200	Invitrogen
Alexa Fluor (568)	anti-Mouse	1:200	Invitrogen
TOM20	anti-Rabbit	1:10 000	Promega

Table 5. List of nuclear markers

Product	Staining concentration	Manufacturer
DRAQ5	1:1250	Cell signalling
DAPI	1:1000	Sigma aldrich

3.5 Imaging and image analysis

Microscopes

An ordinary wide field microscope illuminates the entire sample, therefore, light that reaches the detector is coming from all focal planes, causing the image to blur. To remedy this problem, a confocal microscope contains a pinhole to block out the "out of focus" light from reaching the detector, resulting in sharp images. In addition, confocal microscopy allows for taking images at different optical planes. This optical sectioning, in turn, can be used to build a 3D image with a computer.

The slides are imaged using a regular fluorescent microscope and a confocal microscope (Leica TCS SP5, Wetzlar, Germany). Images are analysed with BioimageXD (Kankaanpaa, Paavolainen et al., 2012).

Segmentation analysis with Bioimage XD

Immunofluorescent images were analysed using Bioimage XD. Segmentation analysis was done in order to calculate the number of insulin vesicles per cell and to compare the number of insulin vesicles in keratin positive cells to the number of insulin vesicles in keratin negative cells. For each cell the procedure list was the same. A median filter was applied to reduce background noise, and manual thresholding was done to separate the image from the background. In order to ensure that the manual thresholding was consistent, ten images of cells (one cell per image) were analysed three times on different days and the average segmentation result was used for each cell, I.e. the same images of ten cells were analysed on e.g. Monday, then again Tuesday and Wednesday. On each day, the segmentation analysis was recoded and after the 3rd day the average segmentation result was used. The next procedure was object separation, followed by analysing the segmented objects (in this case the insulin vesicles). The results were tabulated on an excel graph and the results were used in GraphPad prism 5 to create a graph (GraphPad, CA, USA). Note that the experiment was done three times, i.e. creating three slides that were stained for insulin, keratin and nuclei. From each slide, five keratin positive cells and five keratin negative cells were randomly chosen and imaged.

3D projections of mitochondria and assessing mitochondrial fragmentation

The stained MIN6 cell samples are imaged using a Leica TCS SP5(Leica, Wetzlar, Germany) confocal microscope. After this, Bioimage XD is used to make 3D projections of the mitochondria. These then are blindly analysed by two different people and graded on a scale from 1-5, 1 being no fragmentation and 5 very fragmented appearances.

Statistical analysis

Analysis of western blots is done using Image J (National Institute of Health, Bethesda, MD, USA), and statistical analysis is done using GraphPad prism 5 (GraphPad Software, La Jolla, CA, USA). Student's t-test, or one-way ANOVA and Bonferroni post-hoc test were used as appropriate.

4. RESULTS

4.1 Increased mitochondrial fragmentation and decrease in mitochondrial protein levels in $K8^{-/-}$ β-cell

In order to study the structure and shape of mitochondria, transmission electron microscopy (TEM) images of mitochondria were obtained by members of our lab (Alam et al., 2013; Silvander et al., 2017). From the TEM images, we can observe notable differences between $K8^{+/+}$ and $K8^{-/-}$cells (see figure 7). The $K8^{-/-}$ image looks overall paler, with pale insulin vesicle core and pale mitochondrial outer membrane, as well as, paler cristae. In addition, there appeared to be smaller, rounder mitochondria present, suggesting increased mitochondrial fragmentation. These changes prompted further investigation into the causing factors of these observations.

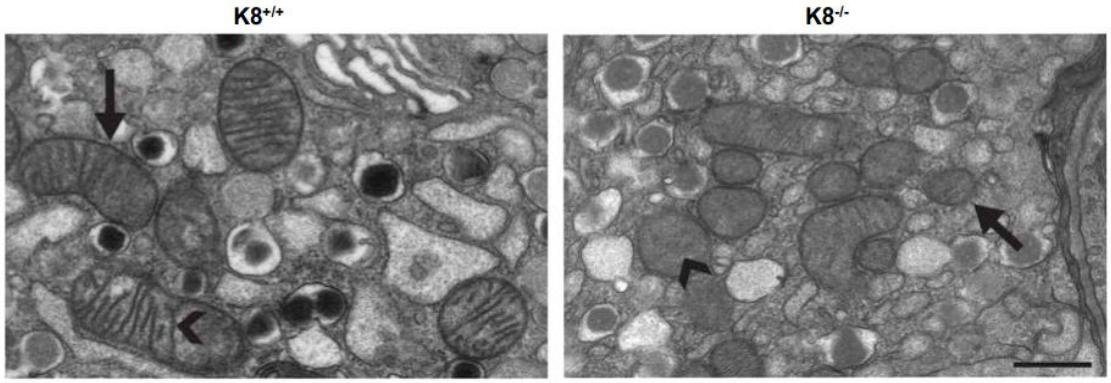

Figure 7. TEM images of islet **β**-cells. Electron microscopy showed altered mitochondrial structures in $K8^{-/-}$ mice, scale bar = 500nm (Alam et al., 2013).

First, mitochondrial fragmentation was assessed by staining primary β-cells with TOM20 (a mitochondrial membrane marker), and obtaining 3D images with a confocal microscope. The 3D images were saved, randomised and blindly analysed by two individuals for the level of fragmentation that was observed in each individual image of a cell. The fragmentation was graded from 1 to 5, where 1 meant that the mitochondria appeared very fused and 5 was assigned to mitochondria that appeared fragmented. Each "dot", in the figure below (Figure 8), represents an individual image of a mitochondria, and the level of fragmentation that was observed. Overall, $K8^{-/-}$ mitochondria appeared to exhibit increased fragmentation compared to $K8^{+/+}$ mitochondria (Figure 8).

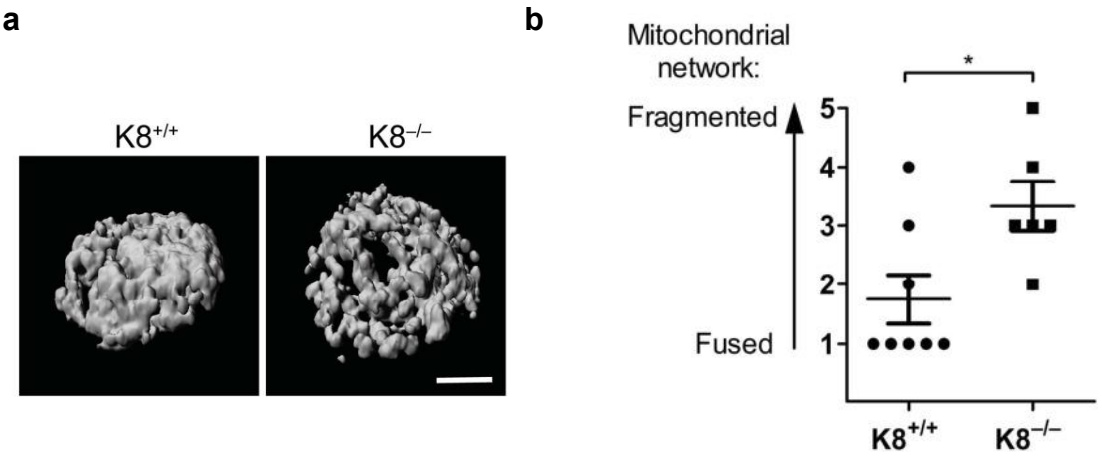

Figure 8. Increased fragmentation of $K8^{-/-}$ MIN6 cells compared to $K8^{+/+}$ MIN6 cells. a: 3D projections of mitochondria, stained with TOM20 (a membrane marker), showed increased fragmentation and unorganized mitochondrial network in $K8^{-/-}$ β-cells. Scale bar = 5 µm b: Quantification of 3D projections by evaluating the degree of mitochondrial fragmentation (by assigning scores ranging from 1= fused to 5= fragmented), evaluated by blind analysis. Note that $K8^{-/-}$ appeared more fragmented. n= 3 mice per genotype. *= $p< 0.05$ average ± SEM.

Decrease in protein levels of MFN2 and TCHP, involved in mitochondrial fusion in $K8^{-/-}$ cells

Mitochondrial fragmentation was further studied by assessing the level of proteins that have been reported to be involved in mitochondrial fusion, such as Mitofusin 2 (MFN2) and OPA1. In addition, the levels of Trichoplein (TCHP), a keratin binding protein, was quantified. For this purpose, mice were sacrificed and pancreatic lysates were isolated and western blotting was done for MFN2 and OPA1. The results (see Figure 9) showed a statistically significant decrease in MFN2 and TCHP protein levels in keratin negative cells compared to keratin positive cells (see Figure 9) , and this is what we had expected. On the other hand, no statistically significant change was observed in the levels of OPA1 in keratin negative cells when compared to keratin positive cells, contrary to what we had expected and what was reported by Zhang et al. (2011).

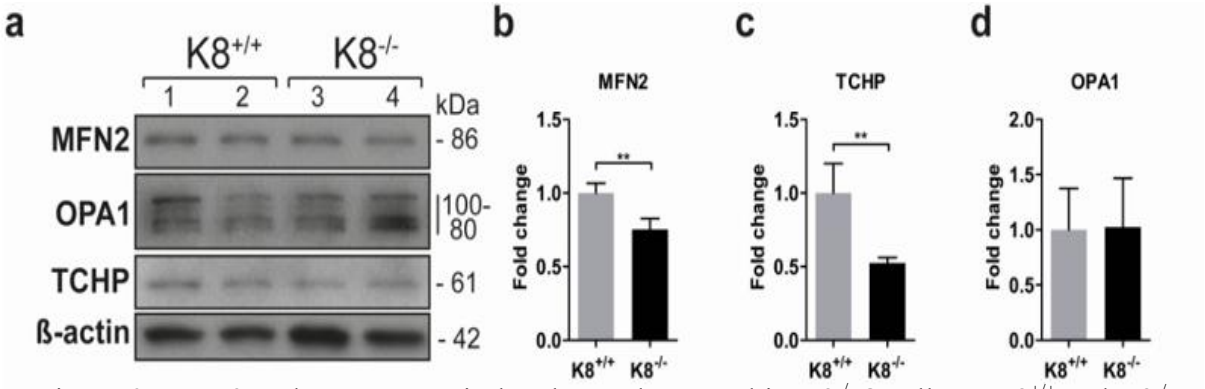

Figure 9. MFN2 and TCHP protein levels are decreased in K8$^{-/-}$ **β**-cells. a: K8$^{+/+}$ and K8$^{-/-}$ isolated islets immunoblotted for MFN2, TCHP, K8 and β-actin (n=4). b: Quantification shows decrease in MFN2 protein amount in K8$^{-/-}$ β-cells, which could lead to a decreased fusion of mitochondria. c: TCHP is decreased approximately 50% in K8$^{-/-}$ β-cells, suggesting that keratin levels affect the linker TCHP. d: OPA1 shows no significant change.Data is shown as average ± SEM **= $p< 0.01$.

Decrease in mitochondrial proteins involved in the electron transport chain in K8$^{-/-}$ cells

Since TEM images of K8$^{-/-}$ β-cells appeared to have a diffuse cristae, we next decided to look into the protein levels of the enzymes involved in the electron transport chain as the proteins associated with it are located in the mitochondrial cristae. This was done by western blotting analysis of mitochondrial complexes I-IV, and for cytochrome c. The results showed (Figure 10) that, as expected, the levels of mitochondrial complexes I and IV, in K8$^{-/-}$ β-cells, were decreased, as well as levels of total mitochondrial cytochrome c were decreased, coinciding with the hypothesis that paler K8$^{-/-}$ mitochondrial cristae could have a reduced amount of mitochondrial complex proteins. This could suggest an inefficient electron transport chain in K8$^{-/-}$ β-cells. However, surprisingly, no decrease was seen in complexes II, III and V.

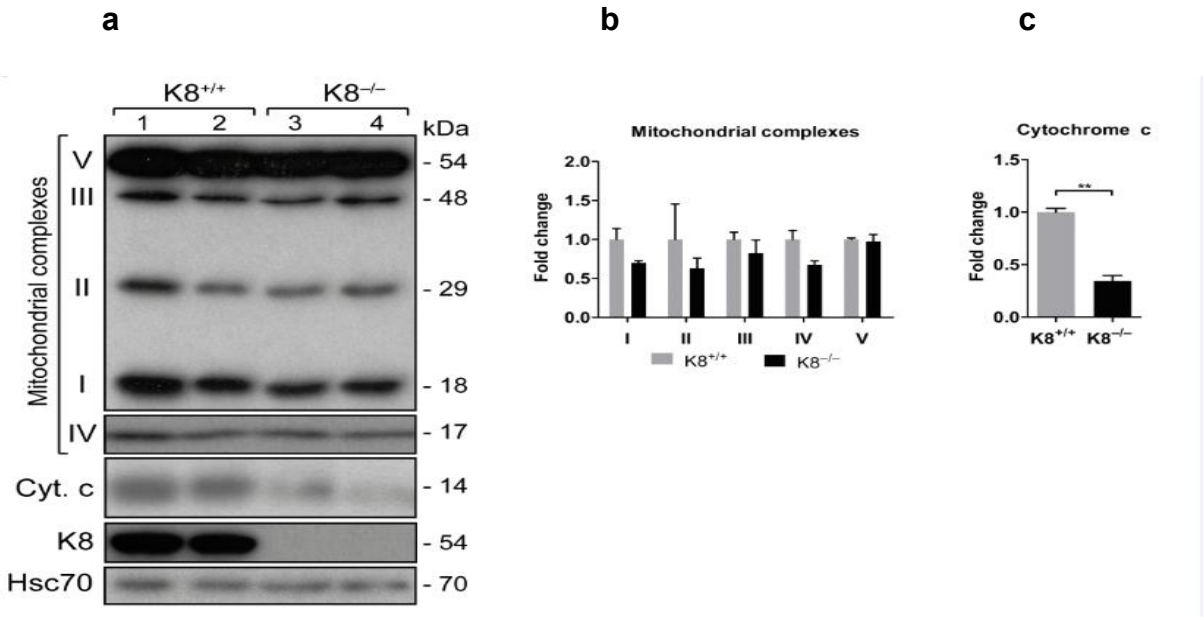

Figure 10. Decreased levels of mitochondrial inner membrane proteins involved in the electron transport chain a: Western blots of isolated $K8^{+/+}$(lanes 1-2) and $K8^{-/-}$ (lanes 3-4) islet lysates for mitochondrial complexes I-IV, total cell cytochrome c, K8 and Hsc70 are shown. n =4 with 2 mice per gel lane. b: n=2, b-c: Western blot quantification of mitochondrial complexes I-V and total mitochondrial cytochrome c, using Hsc70 as a loading control. Data is shown as average ± SEM ** = $p < 0.01$

4.2 Electroporation is the most effective method for transfecting K8/K18 plasmids into MIN6 cells

The MIN6 inuslinoma cell line was chosen as a model for studying keratins in β-cells, as they are an insulin-producing cell line that lacks keratins (K8 $^{-/-}$). This allows for selectively transfecting desired keratins into some MIN6 cells while allowing observation of cells without keratins. In order to be able to compare and contrast K8$^{+/+}$ and K8 $^{-/-}$ cells, keratins first had to be transfected into MIN6 cells. For this purpose, different transfection methods were tested to find out the optimal transfection method for transfecting keratin plasmids into MIN6 cells. The first method used was electroporation, and this is the method that had been previously used by our lab for transfection. Electroporation can be performed on cells with high confluence (70-90%) or low confluence (30-50%). We were interested in imaging individual cells, and thus, a lower confluence was chosen. In addition, this saves time, as MIN6 cells divide slowly (and are split only once a week). The resulting images, obtained from electroporation, would have cells that were dispersed and had plenty of space in-between (see figure 11a). In total, four transfection efforts were imaged and analysed, with transfection efficiencies (see figure 11c). Unfortunately, the highest transfection efficiency that was obtained was only 10%. Since electroporation can be stressful to cells, we decided to try a reagent method to see if it would provide us with a higher transfection efficiency. The chosen method was Lipofectmine 3000. This method, however, required high confluence of the cells (70-80%) and, thus, in the resulting images, the cells appear to be clumped together with very little space in-between them. Unfortunately, the highest transfection efficiency obtained with this method was about 5- 8%. Double transfection was also tried, where the cells were transfected again after 6 or 8 hours, however, this also did not yield a better transfection efficiency.

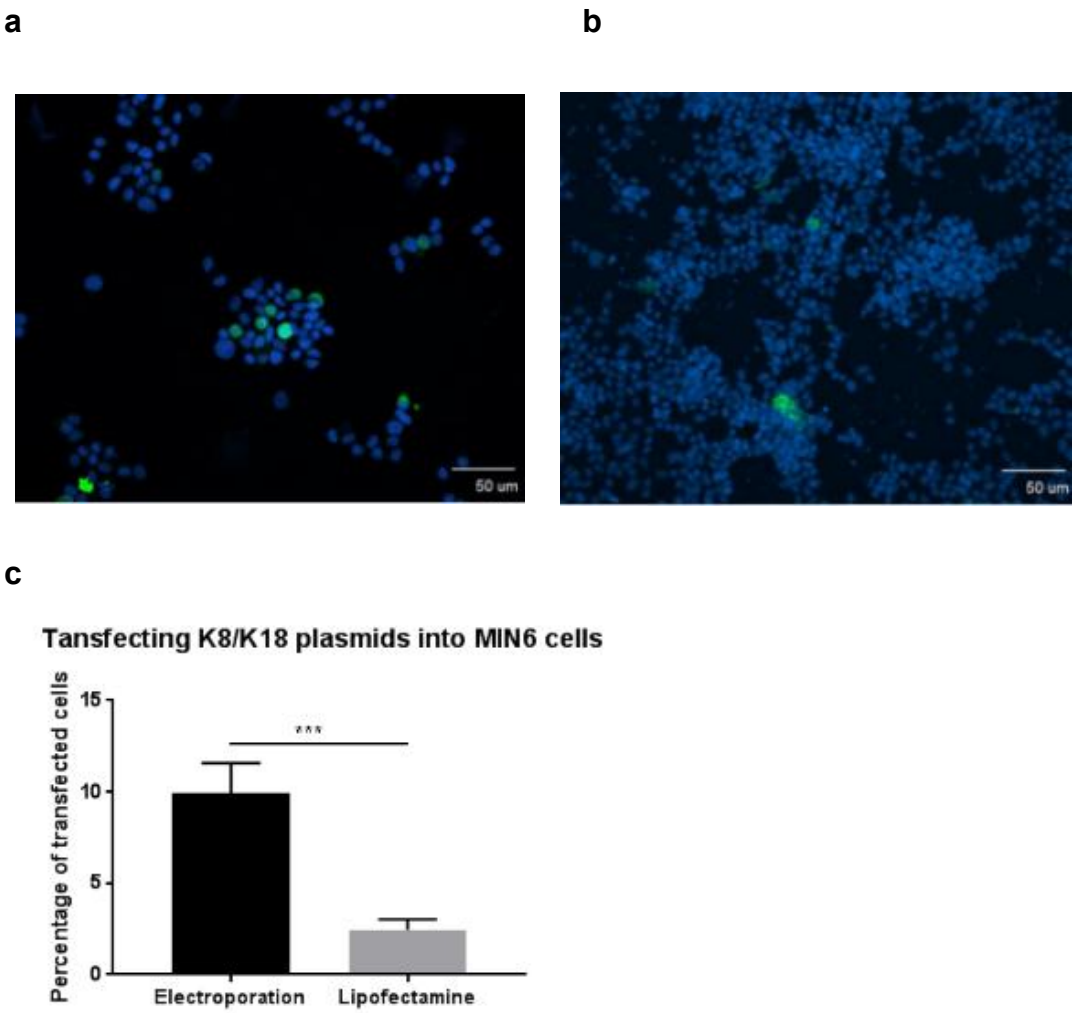

Figure 11. Electroporation is the most effective method for transfecting K8/K18 plasmids into MIN6 cells. a: Transfection by electroporation. Imaged with 3i spinning disk, 20 X magnification, scale bar = 50 µm. b: Transfection by Lipofectamine 3000. Blue channel: nuclei and green channel: keratins. Imaged with 3i spinning disk, 20 X magnification, scale bar = 50 µm. Note that electroporation achieved the highest transfection efficiency of approximately 10% (in this case 8 positive cells out of ~90). No transfection method was able to achieve the desired transfection efficiency of over 50%. c: Percentage of MIN6 cells transfected with keratins, n=4 transfection trials. ***=$p<0.0008$ ± SD.

4.3 Keratin positive MIN6 cells contain more insulin vesicles than keratin negative cells

In order to investigate the amount of insulin vesicles in $K8^{+/+}$ vs. $K8^{-/-}$ cells, MIN6 cells that were transfected with K8/K18 plasmids were stained for insulin, keratins and for nuclei. The insulin stain was placed on the green emission (488 nm) channel, the keratin stain on the red (546 nm) channel and the nuclear stain DAPI emitted at the far red channel, shown as blue. Different staining timings were performed in order to optimise staining. The keratin stain was bright even with only 1 hour of incubation with primary and secondary antibody. However the signal from insulin was weaker and therefore an

overnight staining was done for the keratin stain. This, however, did not affect the quality of staining much as it resulted in more background noise (unspecific staining). Therefore, we continued staining with primary antibodies for just 1 hour. The resulting images can be viewed in figure 12. Both images are from the same slide, i.e from the same slide keratin positive cells were imaged, as well as keratin negative cells. 3D images were used for segmentation analysis. The results show that there are more insulin vesicles in keratin positive cells compared to keratin negative cells (figure 12). This confirms a previous study, where total insulin content of β-cells was measured and it was higher in keratin positive mice (Alam et al., 2013).

a b

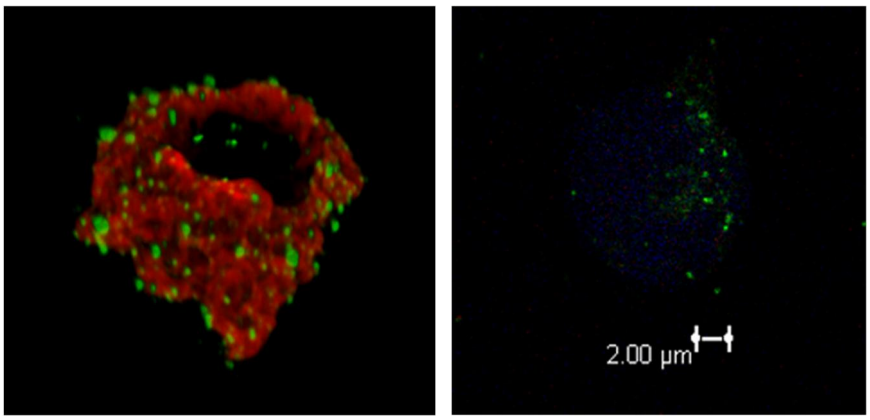

c

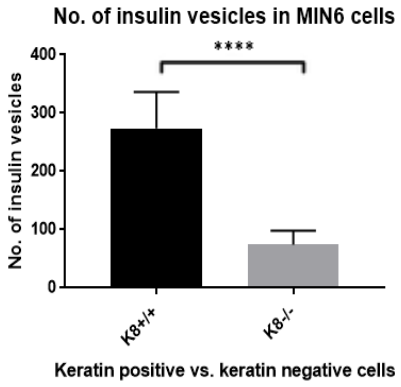

Figure 12. 3D images of a: K8$^{+/+}$ and b: K8$^{-/-}$ MIN6 cells. Segmentation analysis showed K8$^{+/+}$cells contain more insulin vesicles. 3D segmentation analysis (performed using BioimageXD) of MIN6 cells transfected with K8/K8 and stained for keratins (red), insulin(green) and nuclei (blue). 1 cell per image. **c**: Quantification showed that the keratin positive cells contain more insulin vesicle. Graph showing results of 1 slide. 10 images for the slide were obtained. 5 keratin positive cells and 5 keratin negative cells. ****= $p < 0.0001$ ± SD. Note: Nucleus omitted for better view in K8$^{+/+}$ cell.

4.4 Keratin vesicles appear to be lining keratin filaments in MIN6 cells

To determine the position of insulin vesicles in relation to keratin filaments, the same slides, from the previous aim, were used and 2D images were obtained of keratin positive MIN6 cells (see example image in figure 13a). Calculating, whether or not insulin vesicles were lining the keratin filaments, was done manually. The same images were analysed by three individuals and the number on insulin vesicles lining and not lining was calculated (see figure 13b). Visual observation of individuals noted that. it appeared that most of the insulin vesicles were lining the keratin filaments and the statistical results confirmed this observation.

a b

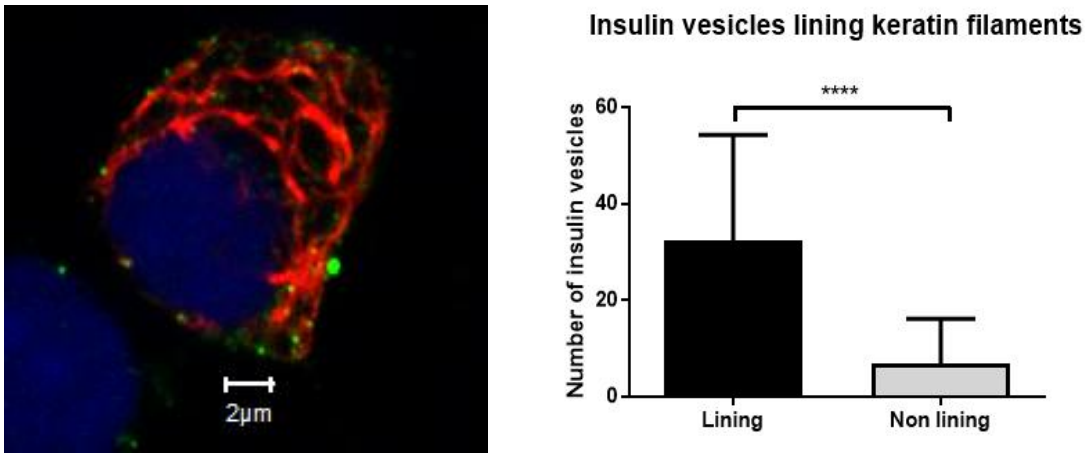

Figure 13. Most of the insulin vesicles are lining the keratin filaments in $K8^{+/+}$ **β**-cells. a: 2D confocal images of MIN6 cells were analysed for insulin vesicles lining the keratin filaments. b: Quantification of the data shows that most of the insulin vesicles appear to be lining the keratin filaments. Data shown as no. of insulin vesicles per cell. Number of cells analysed= n=9, ****= $p < 0.0001$ ± SD

5. DISCUSSION

The pancreas is a fascinating organ which has a dual functionality as both exocrine and endocrine organ. As the organ that is implicated in the development of diabetes, it has been of great interest for further research in investigating its role in the pathophysiology of diabetes. However, very little is known of the role that the cytoskeletal components, keratins, have in the normal functioning of the pancreas. As β- cells of the pancreas are the cells specifically implicated in Diabetes Mellitus (type 1) (Cantley and Ashcroft et al., 2015), these cells were studied. More specifically, we decided to investigate the interaction (or lack thereof) of keratins, mitochondria and insulin vesicles. Both of these β-cell components appeared to have been altered in response to keratin knock out studies (Alam et al., 2013) and, as such, these two components of the β-cells were of great interest and the target of further study.

The aim of this study was to investigate the potential effect of keratins on mitochondria and insulin vesicles in the normal homeostasis of the β-cells of the pancreas and, in doing so, identify a possible pathological mechanism contributing to the lack of insulin production leading to diabetes. Furthering our understanding in this area is crucial, as so far studies have not shown conclusively how mitochondria and insulin vesicles are affected by keratins. The hypothesis was that keratins are important for normal mitochondrial homeostasis and insulin production in β-cells.

5.1 Increased fragmentation of $K8^{-/-}$ mitochondria and decrease in mitochondrial protein levels

In a previous study done by electron microscopy by our laboratory (Alam et al., 2013), mitochondria in $K8^{-/-}$ β-cells appeared to be morphologically different compared to $K8^{+/+}$ β-cells. In their study, electron micrographs were taken, where $K8^{+/+}$ cells appeared to have elongated and larger mitochondria, whereas $K8^{-/-}$ β-cells showed rounder, smaller and perhaps fragmented mitochondria. In this study, we further analysed these observations by staining mitochondria using TOM20 (a mitochondrial outer membrane protein) and labelling for fluorescence microscopy. Confocal microscopy imaging allowed for z-stacks to be created allowing for 3D visualization, scoring and quantification of the mitochondrial outer fragmentation. This, in turn, reaffirmed the

observations that were made by Alam et al. (2013). Indeed, the mitochondria in $K8^{+/+}$ cells appeared to be more fused than the $K8^{-/-}$ cells. This proposes a potential link between mitochondria and keratins, emphasising that keratins do, indeed, play a role in normal $K8^{+/+}$ β-cell homeostasis. These findings correspond to those made by Tao et al. (2009) in liver and Gentil et al. (2012) which reported that K8 was involved in morphological alterations of mitochondria.

It is noteworthy that mitochondrial fusion and fission are important processes by which the cell can, for example, remove defective components, respond to cell stress and meet cellular demands (Liesa and Shirihai 2013).

Fragmentation is associated with defective mitochondria, and is often observed in instances such as during apoptosis or defective OXPHOS (Molina et al. 2009; Tagaguchi et al. 2007). MFN2, TCHP and OPA1 are all proteins that are involved in mitochondrial fusion and, therefore, these proteins were targets of interest as their levels could be used as flag bearers for the observed mitochondrial fragmentation. TCHP is a cytolinker that binds keratins to MFN2 (Cerqua et al. 2010). The results showed a significant decrease (50%) in TCHP protein levels in $K8^{-/-}$ cells compared to $K8^{+/+}$ cells, pointing towards the involvement of the TCHP in mitochondrial fragmentation.

In addition, as we expected, MFN2 levels were decreased (by 25%) in $K8^{-/-}$ β-cells. This reaffirms observations made previously and points towards a possible reason behind the observed fragmentation, as the binding of MFN complexes on mitochondria is crucial in order for the fusion process of mitochondrial double membrane to occur. These findings coincide with those of deBritto and Scorrano (2008) which reported reduced levels of MFN2 and fragmentation of the mitochondrial network of HeLa cells.

Finally, OPA1 levels were observed and surprisingly the levels appeared to be the same for both $K8^{-/-}$ and $K8^{+/+}$ cells, unlike what we had expected. We had anticipated a decrease in OPA1 levels, as this is an important fusion protein and another study had associated the lack of OPA1 with mitochondrial fragmentation (Zhang et al., 2011).

Mitochondrial inner membrane protein level analysis

A study done in our laboratory (Alam et al., 2013) that showed morphological differences in mitochondria between $K8^{-/-}$ and $K8^{+/+}$ cells, also showed the overall appearance of cristae to be seemingly paler (Alam et al., 2013). Therefore, several proteins found in the

inner membrane that is part of ATP production and the electron transport chain (OXPHOS cycle) were further studied by western blotting and we hypothesised that the protein levels of all or some of the proteins would be decreased. As was predicted, a small decrease was seen in OXPHOS complexes I and IV, whereas complexes II and III remained unaltered in $K8^{-/-}$ cells compared to $K8^{+/+}$ cells. Interestingly, Cytochrome c was significantly reduced in $K8^{-/-}$ cells. These proteins are involved in the normal functioning of the mitochondria and, thus, any changes could signal a possible adverse alteration and point towards perhaps an insufficient electron transport chain in $K8^{-/-}$ cells. This once again highlights the importance of keratins in the β-cells.

5.2 Electroporation is the most effective method for transfection of K8 into MIN6 cells

In order to image and study keratins and insulin vesicle intracellularly we needed another model for cellular studies of keratins. To do this, keratins had to be first transfected into MIN6 cells. For this purpose, different transfection methods were tried in order to optimise transfection, as the MIN6 cell line does not have ready protocols and is notorious for being a difficult cell line to transfect (Muller et al., 2010). The keratins to be transfected into the MIN6 cells were K8 and K18, as these have been shown to be the keratins that are present in the β-cells of the pancreas (Alam et al., 2013). Two transfection methods were chosen: reagent based and electroporation. Our lab had been using electroporation and the highest transfection efficiency reported was 10%. However, electroporation relies on electric shock that will temporarily fragment the cell membrane and is therefore stressful for the cell and can be a source of cell damage. Therefore, our aim was to explore an alternative transfection method which could also produce transfection efficiency much higher than 10%. Several studies had reported using Lipofectamine (Hardy et al., 2015; Calabrese et al., 2003), so we opted for trying it. In our case, we opted for using Lipofectamine 3000 (Thermofisher) as it was seen as the superior and updated version of Lipofectamine due to having an extra reagent addition step in its protocol with the aim of improving transfection efficiency. We had hypothesised that by using this method we would be able to obtain at least a transfection efficiency of 30%. Unfortunately, this was not the case and, at best, the transfection efficiency was 10%. This was the case whether the Lipofectamine 3000 reagent used was 3.7µl or 7.7µl. Double transfection was also tried in the hope of increasing the transfection efficiency but did

not improve the efficiency. Other studies did not mention their transfection efficiencies, but there were mentions of difficulties with transfecting into MIN6 cells (Han et al., 2007; Torii et al., 2002; Rfiq, Kennedy and Rutter 2018) in other studies. Therefore we decided to proceed with the transfection efficiency of 10% which was sufficient for microscopy assays, since transfected and non-transfected cells could be distinguished from each other since fluorescently tagged keratin constructs were used.

Electroporation was chosen as the transfection method as it allowed for transfection at a lower cell confluence, allowing for better visualization of individual cells, necessary for imaging assays. Confluence played an important role when it came to deciding on a transfection method, as our aim was to image individual cells and electroporation only required a confluence of 50-60% for transfection, making imaging cells easier compared to Lipofectamine 3000 which required a confluence of 70-80% resulting in clumping of cells, obstructing the view and prohibiting good visualization of individual cells.

5.3 $K8^{+/+}$ MIN6 cells contain more insulin vesicles than $K8^{+/+}$ cells

A previous study by our laboratory (Alam et al., 2013) reported higher total insulin amount in keratin wild type cells compared to keratin knock out cells. To confirm these findings and to further investigate if this was the case also on an individual cellular level, individual cells were imaged for their insulin content. Segmentation analysis of individual MIN6 cells was done with BioimageXD and it confirmed our hypothesis that $K8^{+/+}$ cells have higher amount of insulin vesicles (and hence insulin amount) per cell compared to $K8^{-/-}$ cells MIN6 cells. This further enforces the results shown previously by our lab and supports the hypothesis that keratins are important in β-cell insulin regulation and/or secretion. As presented by Alam et al., (2013), keratins have multiple functions in the mouse endocrine pancreas and other studies have also reported the importance of the cytoskeleton in insulin regulation. In particular, actin and microtubules have previously been reported to play a role in insulin secretion and release (Lacy et al., 1972 & Ori et al., 1972). However, the only published study looking specifically at a causal link between keratins and insulin secretion to date has been the study by Alam et al., 2013. Interestingly, a study by Wijeskara et al., (2010) looked into the effects of Znt8 deletion in mice and their results showed resemblance to ours. Interestingly they reported that β-cell specific deletion of Znt8 resulted specifically in reduced 1st phase insulin response. In addition, they report altered insulin vesicle morphology which could also

contribute to the alteration of insulin levels in knockout cells. It would be interesting to see if keratin deletion would also affect zinc or Znt8 levels and to see if the two are linked. Indeed, the pale insulin vesicle cores seen previously by our lab (Alam et al., 2013) could be due to reduced zinc levels caused by a keratin deletion in β-cells.

Segmentation analysis as a method of quantification of insulin vesicles and use of Bioimage XD

Image analysis can be done in many different ways depending on the needs and resources. It is a crucial part of research which involves imaging in many forms (microscopy, TEM, MRI etc). With the help of various bio-imaging software available, it is possible to extract important and useful information from images. For the purpose of this research, a free imaging software was needed which was readily available for use. The bioimaging software chosen was Bioimage XD (Kankaanpaa et al., 2009). This is because unlike ImageJ/Fiji (which is also an open source bioimaging software), Bioimage XD concentrated on multidimensional images. In addition, Bioimage XD is especially developed for visualisation of fluorescent microscopy and, as the images obtained in this study were fluorescent 3D images of cells, this software was seen as the optimum choice. Segmentation analysis was chosen as the most appropriate method for quantification of insulin vesicles. The most important aspect of image analysis is reduction of personal bias and making sure the images are not incorrectly altered in a way which would disturb the validity of the results. As manual thesholding was used as part of the segmentation analysis, in order to eliminate personal bias and to ensure consistency, the first 10 images were analysed three times on three different days.

5.4 Insulin vesicles lining keratin filaments

While imaging MIN6 cells (that were transfected with keratins) for insulin content, an interesting phenomenon was observed. Fluorescently labelled keratins appeared to be lining keratin filaments. With this in mind, the experiments were repeated and the same phenomena appeared once again. Fluorescent images were obtained and image processing was used to try to enhance the image quality and to be able to discern more clearly the association of keratins and insulin vesicles. However, it is difficult to tell how the insulin vesicles are associating with the keratins. We are limited by the resolution of

the images at hand and the dyes and staining techniques that we used to our best knowledge. With the information at hand it is difficult to say how close the insulin vesicles are to the keratin filaments and, furthermore, how they are associated.

As there are no other specific studies done on the interaction between keratins and insulins, it is difficult to evaluate or compare our findings. Thus, we are only able to hypothesise if and how this phenomenon is occurring. Indeed, it is plausible that keratins would associate with insulin vesicles, as there are several cyto-linkers that bind keratins such as TCHP and plectin (Liffers 2011: Nishizawa 2005; Winter 2008) that could potentially act as linkers in this case as well. Other proteins could also be considered to have a potential role in the insulin vesicle-keratin association. Several proteins are known to be involved in insulin vesicle release (Wang and Thurmond 2009) and any of these proteins could pose as potential candidates for future research.

6. CONCLUSIONS

1) Investigate the role of keratins in pancreatic β-cell mitochondrial fusion and fission

From the results presented here, combined with previous research, it can be concluded that keratins are important for mitochondrial fusion and homeostasis, seeing how there is an increased fragmentation in K8 knock out mice and a decrease in mitochondrial protein levels in the absence of K8.

2) Determine the best transfection method for transfecting K8/K18 into MIN6 cells

For the purpose of this study, where imaging individual cells was desired, electroporation was the most appropriate transfection method, and one that yielded the highest transfection efficiency (10%).

3) Investigate insulin vesicle regulation

Keratins play an important role in insulin vesicle regulation. This is illustrated by the fact that the $K8^{-/-}$ β-cells contain less insulin vesicles and by the results from 2D analyses of immunfluorescent images showing insulin vesicles lining keratin filaments.

7. ACKNOWLEDGMENTS

Firstly, I would like to express my deepest gratitude to Diana Toivola for accepting me to do my internship and consecutively my Master´s Thesis in her lab and, for the continuous guidance and inspiration throughout my time in the lab. In addition, I would like to thank my supervisor Jonas Silvander, for teaching me all the lab skills I have acquired, for the valuable knowledge and guidance and Catharina Alam for reading my thesis and giving me valuable comments to improve it.

Finally, I would like to take this opportunity to thank all the members of Diana Toivola Lab that provided me with an amazing environment for working and learning. Julia, Terhi, Iris, Linda, Laura, Kalle and Joel, thank you for being the happy and hard working people that you are.

Thank you!

8. APPENDIXES

8.1 Image analysis protocol: Segmentation analysis of insulin vesicles

In order to quantify the number of insulin vesicles per cell, segmentation analysis was performed on each 3D image stack.

1) Folder(s) containing images is opened in BioimageXD. All channels are selected and are merged to show all of the stains. Each 3D stack is looked through to check the quality of the imaging (e.g. to see if there is any over exposure).

   To open a folder: click “open data set” 

   From the file tree, select all channels and click “merge”

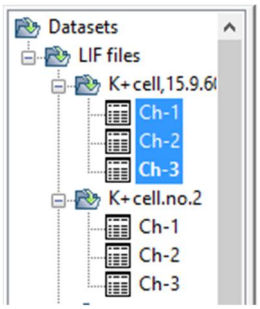

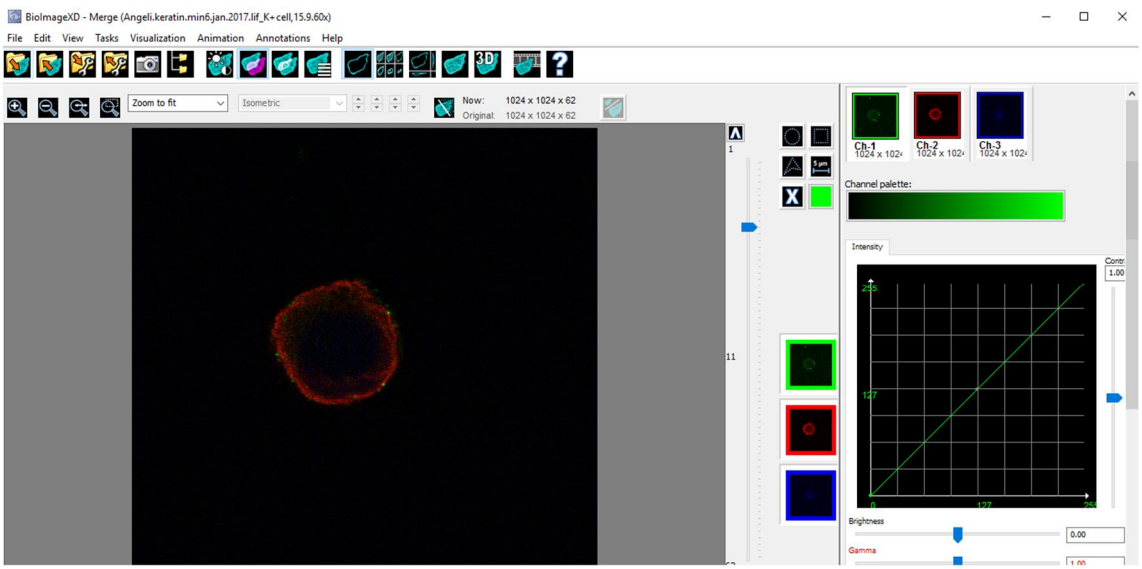

2) Background noise is removed by using a median filter. The median works by replacing each pixel or voxel in this case as we are working with 3D images, with a median value inside the kernel (BioimageXD). This method was chosen because each number in the kernel is replaced by a median number, and therefore this method is much less sensitive to outliers, and, thus it is better at preserving edges (i.e less blurring).

Click on  “procedure list” filtering -> noise removal -> Median

3) Thresholding is used in order to separate the insulin signal from the background. Since the insulin stain produced some degree of background noise (unspecific binding), manual thresholding was done.
(In order to ensure that the manual thresholding was consistent, the first 10 images were analysed 3 times on 3 different days: I.e. Day 1. Image analysis of images 1-10, day 2. Image analysis if images 1-10 and the same for day 3. Following this, the average for each image was noted and used for statistical analysis. Since the values were consistent, for the rest of the images, image analysis was performed only once.)

	A	B	C	D	E	F	G	H	I	J	K	L
1		K+(cell1)	K+(cell2)	K+(cell3)	K+(cell4)	K+(cell5)		K- (cell6)	K-(cell7)	K-(cell8)	K-(cell9)	K-(cell10)
2	No. of in:	250	303	377	217	200		50	30	97	80	60
3		276	330	374	223	208		62	53	93	110	80
4		292	315	326	225	191		54	50	102	90	100
5	Average:	273.6	316	356	221	199		55	44	97	93	80
6												

4) Object separation is used with settings of: segmentation level 1 and remove objects with less voxels than 3.

Segmentation -> Object processing -> Object separation

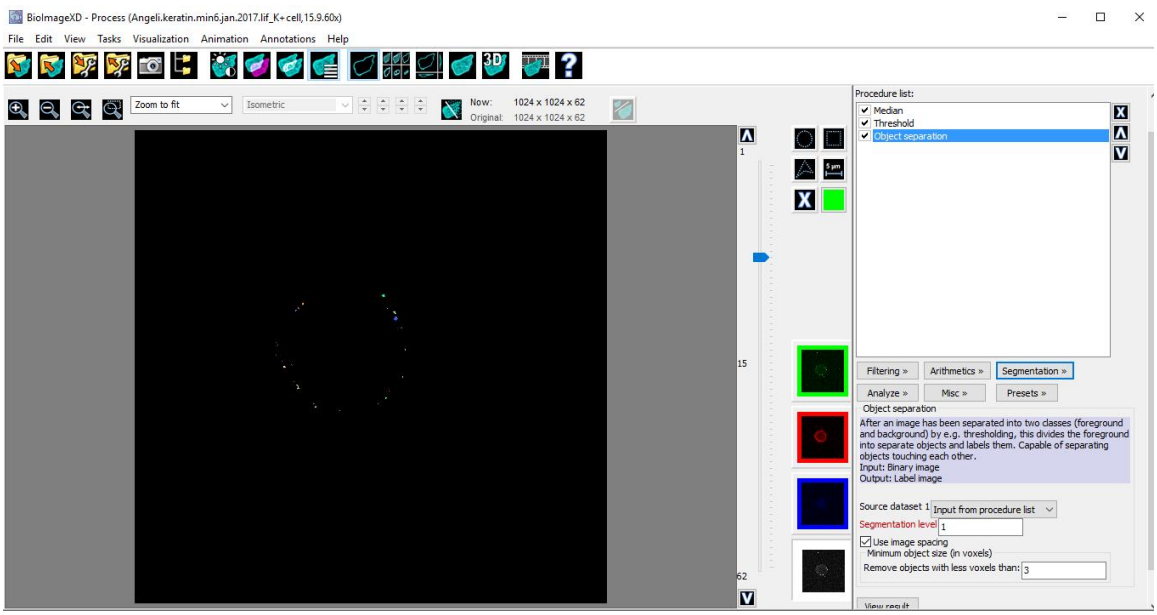

5) The final step is to analyse the segmented objects. The value for no. of objects is noted down and the same procedure is repeated for the next image.

Analyse -> segmentation-based analyses-> analyse segmented objects

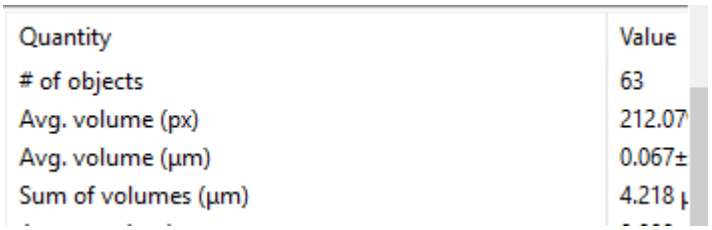

Quantity	Value
# of objects	63
Avg. volume (px)	212.07
Avg. volume (µm)	0.067±
Sum of volumes (µm)	4.218 µ

8.2 Recipes and protocol

Western blotting

10x running buffer for SDS-page

120 g	Tris-Base
576 g	Glycine
Up to 4l	MQ-H_2O

Transfer buffer

Amount	substance
160 ml	running buffer
1440 ml	DT- H_2O
200 ml	Methanol
1 ml	20% SDS

SDS-separating gel with varying amount of acrylamide concentration (10-12%)

Immunofluorescence staining

Buffer A

2,5% BSA in 1x PBS

Buffer B

200 ml	Buffer A
1:50	Normal goat serum
1:50	Normal donkey serum

0,2 % NP+40

5 ml 1x PBS

10 ul NP-40 (Sigma-Aldrich)

Cell culture medium for MIN6 cells

600 ml DMEM (Dulbecco's Modified Eagle's Medium)

6 ml 15% Foetal calf serum (Biowest)

6 ml sodium pyruvate,

6 ml 1% penicillin (Gibco)

6 ml GlutaMax

14.5% β-mercapto ethanol

8.3 Transfection of MIN6 cells by using a reagent method: Lipofectamine 3000 and staining for insulin and keratins 20.05.2016

The aim of Lipofectamine transfection is so that we can stain for keratins and insulin on MIN6 cells that were transfected by Lipofectamine and compare this to cells that were electroporated.

The protocol used was the protocol given by the company.

Cells were seeded on to a 24well plate with glass slides until a confluency of 70% was reached. Following this 4 wells are used to study the transfection efficiency.

Each well will contain:
1.5 µl Lipofectamine 3000 reagent 25 µl Optimem 2 µl P3000 reagent 5 µg K8 (non-fluorescent) 5 µg K18 (non-fluorescent)

Protocol:

1. Change media of cells (each well=500µl media)

2. In and eppendorf tube add:

- 250µl Optimem

- 14µl Lipofectamine

3. In another eppendorf tube add:

- 250µl Optimem

- 7µl K8 and 10µl K18

- 10µl P3000 reagent

4. Mix solutions from 2 and 3 and incubate for 5 min in room temperature.

5. Add the solution to 24 wells plate. 25µl per well.

REFERENCES

Alam, C., Silvander, J., Daniel, E., Tao, G., Kvarnstrom, S., Alam, P., Omary, M., Hanninen, A. and Toivola, D. (2013) Keratin 8 modulates β-cell stress responses and normoglycaemia. Journal of Cell Science. 126:5635-5644.

Alberts, B., Johnson. A., Lewis, J. (2002). Isolating, Cloning, and Sequencing DNA. Molecular Biology of the Cell. 4th edition. New York: Garland Science. Available from: https://www.ncbi.nlm.nih.gov/books/NBK26837/

Alvarao, D.M., and Coulombe, P.A. (2014). Directed expression of a chimeric type II keratin partially rescues keratin 5-null mice. J.Biol.Chem. 289:19435–19447. doi:10.1074/jbc.M114.55386

Anderson, S., Bankier, A. T., Barrell, B. G., de Bruijn, M. H. L., Coulson, A. R.; Drouin, J., Eperon, I. C., Nierlich, D. P., Roe, B. A., Sanger, F., Schreier, P. H., Smith, A. J. H., Staden, R., Young, I. G. (1981). Sequence and organization of the human mitochondrial genome. Nature. 290:457–465.

Asghar, M.N., J.S. Silvander, T.O. Helenius, I.A. Lahdeniemi, C. Alam, L.E. Fortelius, R.O. Holmsten, and D.M. Toivola. (2015) The amount of keratins matters for stress protection of the colonic epithelium. PloS one. 10:e0127436.

Baribault, H., Penner, J., Iozzo, R.V., Wilson-Heiner, M. (1994). Colorectal hyperplasia and inflammation in keratin 8-deficient FVB/N mice. Genes & development. 8:2964-2973

Blanco, Francisco & Rego, Ignacio & Ruiz-Romero, Cristina. (2011). The role of mitochondria in osteoarthritis. Nature reviews. Rheumatology. 7:161-9. 10.1038/nrrheum.2010.213.

Bragulla H.H., Homberger D.G. (2009) Structure and functions of keratin proteins in simple, stratified, keratinized and cornified epithelia. Journal of Anatomy. 214: 516–559.

Berg, J.M., Tymoczko, J.L., Stryer, L. (2002) Biochemistry. 5th edition. New York: W H Freeman; Chapter 18, Oxidative Phosphorylation. Available from:

https://www.ncbi.nlm.nih.gov/books/NBK21208/

Burnette, W.N. (1981) "Western blotting": electrophoretic transfer of proteins from sodium dodecyl sulfate--polyacrylamide gels to unmodified nitrocellulose and radiographic detection with antibody and radioiodinated protein A. Anal Biochem. 112:195-203.

Chamcheu, J. C., Siddiqui, I. A., Syed, D. N., Adhami, V. M., Liovic, M., & Mukhtar, H. (2011). Keratin Gene Mutations in Disorders of Human Skin and its Appendages. Archives of Biochemistry and Biophysics. 508:123–137. http://doi.org/10.1016/j.abb.2010.12.019

Cheng, K., Delghingaro-Augusto, V., Nolan, C.J., Turner, N., Hallahan, N., Andrikopoulos, S., (2012) High Passage MIN6 Cells Have Impaired Insulin Secretion with Impaired Glucose and Lipid Oxidation. PLoS ONE 7(7): e40868. doi:10.1371

Cooper, G.M. (2000) The Cell: A Molecular Approach. 2nd edition. Sunderland (MA): Sinauer Associates; Intermediate Filaments. Available from: https://www.ncbi.nlm.nih.gov/books/NBK9834/

Coulombe, P. A., Ma, L., Yamada, S., Wawersik, M. (2001) Intermediate filaments at a glance. Journal of Cell Science. 114: 4345-4347;

Dany, S., Muller, Peter M. Jones and Shanta J. Persaud. (2006) Expression of a potent anti-apoptotic protein in MIN6 β-cells using METAFECTENE PRO.

Diaz-Valencia, P. A., Bougnères, P., & Valleron, A.-J. (2015). Global epidemiology of type 1 diabetes in young adults and adults: a systematic review. BMC Public Health. 15, 255. http://doi.org/10.1186/s12889-015-1591-y

De Brito, O. M. & Scorrano, L. (2008) Mitofusin 2 tethers endoplasmic reticulum to

mitochondria. Nature 456, 605-610

Elayat, A. A., el-Naggar, M.M., and Tahir,M. (1995) An Immunocytochemical and Morphometric Study of the Rat Pancreatic Islets. Journal of Anatomy. 186. Pt 3: 629–637. Print.

Fu, Z., Gilbert, E. R., and Liu, D. (2013). Regulation of Insulin Synthesis and Secretion and Pancreatic Beta-Cell Dysfunction in Diabetes. Current Diabetes Reviews. 9:25–53.

Gaw, A., Murphy, M., Srivastava, R., Cowan, R. and O'Reilly, D. (2013) Clinical biochemistry. Edinburgh: Churchill Livingstone/Elsevier.

Giles, R., H Blanc, H M Cann, D C Wallace Maternal inheritance of human mitochondrial DNA (1980) Proceedings of the National Academy of Sciences. 77:6715-6719; DOI:10.1073/pnas.77.11.6715

Hales, C. (1997) Non-insulin-dependent diabetes mellitus. British Medical Bulletin. 53: 109-122.

Hatch, A.L., Gurel, P.S., and Higgs, H.N. (2014) Novel roles for actin in mitochondrial fission. J. Cell Sci. 127:4549–4560. doi:10.1242/jcs.15379

Hennekam, R CM. (2006) Hutchinson–Gilford progeria syndrome: Review of the phenotype. Am J Med Genet. Part A 140A:2603–2624.

Helenius, T.O., C.A. Antman, M.N. Asghar, J.H. Nystrom, and D.M. Toivola. (2016) Keratins Are Altered in Intestinal Disease-Related Stress Responses. Cells. 5.

Jitrapakdee, S., Wutthisathapornchai, A., Wallace, J. C., & MacDonald, M. J. (2010). Regulation of insulin secretion: role of mitochondrial signalling. Diabetologia. 53: 1019–1032. http://doi.org/10.1007/s00125-010-1685-0

Jolles, S., (2002). Paul Langerhans. Journal of Clinical Pathology. 55:243-243.

Kahn, S. E., Cooper, M. E., & Del Prato, S. (2014). PATHOPHYSIOLOGY AND TREATMENT OF TYPE 2 DIABETES: PERSPECTIVES ON THE PAST, PRESENT AND FUTURE. Lancet. 383:1068–1083. http://doi.org/10.1016/S0140-6736(13)62154-6

Komatsu, M., Takei, M., Ishii, H., & Sato, Y. (2013). Glucose-stimulated insulin secretion: A newer perspective. Journal of Diabetes Investigation. 4:511–516.

http://doi.org/10.1111/jdi.12094

KU, N.O., Strnad, P., Zhong B.H., Tao, G.z., and Omary, M.B. (2007) Keratins let liver live: mutations predispose to liver disease and crosslinking generate Mallory-Denk bodies. Hepatology. 45:1639–1649

Kim, T. K., & Eberwine, J. H. (2010). Mammalian cell transfection: the present and the future. Analytical and Bioanalytical Chemistry. 397:3173–3178. http://doi.org/10.1007/s00216-010-3821-6

Kumar,V., Bouameur, JE., Bär, J., Rice, RH., Hornig-Do, HT., Roop, DR., Schwarz, N., Brodesser,S., Thiering, S., Rudolf E. Leube, Rudolf J. Wiesner,Vijayaraj,P., Helle., S., Seibel, P., Magin, T.M. (2015). A keratin scaffold regulates epidermal barrier formation, mitochondrial lipid composition, and activity. J Cell Biol Dec 2015, 211 (5) 1057-1075; DOI: 10.1083/jcb.201404147

Lakowicz., J.R. (1999) Principles of Fluorescence Spectroscopy (Second edition), Plenum, New York

Liesa, M., Palacín, M., Zorzano, A. (2009) Mitochondrial dynamics in mammalian health and disease. Physiol Rev. Jul;89(3):799-845. doi: 10.1152/physrev.00030.2008 https://www.ncbi.nlm.nih.gov/pubmed/19584314

Llanos, P., Contreras-Ferrat, A., Barrientos, G., Valencia, M., Mears, D., Hidalgo, C., (2015) Glucose-Dependent Insulin Secretion in Pancreatic β-Cell Islets from Male Rats Requires Ca^{2+} Release via ROS-Stimulated Ryanodine Receptors. PLoS ONE. 10(6): e0129238. https://doi.org/10.1371/journal.pone.0129238

Lowery,. J., Kuczmarski, E.R., Herrmann, H., and Goldman, D.R. (2015) Intermediate Filaments Play a Pivotal Role in Regulating Cell Architecture and Function. Journal of Biological chemistry. doi: 10.1074/jbc.R115.640359jbc.R115.640359.

Malka, F., Guillery, O., Cifuentes-Diaz, C., Guillou, E., Belenguer, P., Lombès, A., and Rojo, M. (2005). Separate fusion of outer and inner mitochondrial membranes. EMBO Reports. 6(9), 853–859. http://doi.org/10.1038/sj.embor.7400488

Martin, W., Roettger, M., Kloesges, T., Thiergart, T., Woehle, C., Gould, S., Dagan, T. (2012) Modern endosymbiotic theory: Getting lateral gene transfer in-to the

equation. Journal of Endocytobiosis and Cell Research. 23: 1–5.

Mayer-Davis, E. J. (2017) Incidence Trends of Type 1 and Type 2 Diabetes among Youths, 2002–2012. N. Engl. J. Med. 376: 1419–1429

Meloni, A. R., DeYoung, M. B., Lowe, C., & Parkes, D. G. (2013) GLP-1 receptor activated insulin secretion from pancreatic β-cells: mechanism and glucose dependence. Diabetes, Obesity & Metabolism. 15:5–27. (http://doi.org/10.1111/j.1463-1326.2012.01663)

Mingming Hao, Xia Li, Mark A. Rizzo, Jonathan V. Rocheleau, Benoit M. Dawant, David W. Piston. (2005) Regulation of two insulin granule populations within the reserve pool by distinct calcium sources Journal of Cell Science. 118: 5873-5884; doi: 10.1242/jcs.02684

Mikhaylova, M., et al. (2015) Resolving bundled microtubules using anti-tubulin nanobodies. Nat. Commun. 6, 7933

Nishizawa, M., Izawa, I., Inoko, A., Hayashi, Y., Nagata. K., Yokoyama, T., Usukura, J., Inagaki, M., (2005) Identification of trichoplein, a novel keratin filament-binding protein. Journal of Cell Science. 118(Pt6): 1081-90.

Olofsson, C.S., S.O. Gopel, S. Barg, J. Galvanovskis, X. Ma, A. Salehi, P. Rorsman, and L. Eliasson. (2002) Fast insulin secretion reflects exocytosis of docked granules in mouse pancreatic B-cells. Pflugers Archiv: European journal of physiology. 444:43-51.

Omary, M., Ku, N., Strnad, P. and Hanada, S. (2009) Toward unravelling the complexity of simple epithelial keratins in human disease. Journal of Clinical Investigation. 119: 1794-1805.

F. John G. Ebling. D.Sc., Ph.D. Homage to Paul Langerhans: Department of Zoology, University of Sheffield, Sheffield, S10 2TN, England. Available online 5 January 2016.

Piper Treuting, Suzanne, Dintzis, Denny Liggit, Charles W. Frevert. (2011) Comparative Anatomy and Histology: A Mouse and Human Atlas; Academic Press Inc, ISBN/EAN:978-0-12-381361-9.

Ross, M. and Pawlina, W. (2011) Histology. Philadelphia: Wolters Kluwer/Lippincott Williams & Wilkins Health.

Rutter, G. (2006) Insulin Vesicle Release: Walk, Kiss, Pause ... Then Run. Physiology, 21(3), 189-196.

Silvander J. S.G., (2018) Keratins in the endocrine pancreas- Novel regulators of cellular processes in β-cells. Åbo Akademi, Turku

Snider N.T., Omary, M.B. (2014) Post-translational modifications of intermediate filament proteins: mechanisms and functions. Nature Reviews Molecular Cell Biology 15: 163–177.

Steinert, P.M., Steven, A.C., Roop, D.R. (1985) The molecular biology of intermediate filaments. Cell. 42:411–420

Straub, S.G., and Sharp, G.W.G. (2004) Hypothesis: one rate-limiting step controls the magnitude of both phases of glucose-stimulated insulin secretion American Journal of Physiology-Cell Physiology 287:3, C565-C571

Stiles, L., & Shirihai, O. S. (2012). Mitochondrial Dynamics and Morphology in Beta-Cells. Best Practice & Research. Clinical Endocrinology & Metabolism. 26: 725–738. http://doi.org/10.1016/j.beem.2012.05.004

Stewart, M.J., Shepherd, J. (2008) Clinical biochemistry: An Illustrated Colour Text

Sun, T.T., Eichner, R., Nelson, W.G., Tseng, S.C., Weiss, R.A., Jarvinen, M. (1983) Keratin classes: Molecular marker for different types of epithelial differentiation. J Invest Dermatol. 81:109s–115s

Suzanne M. Dintzis, Denny Liggitt. (2012) Comparative Anatomy and Histology A Mouse and Human Atlas, Pages 203–209

Svoboda., Karel and Yasuda, R. (2006) Principles of Two-Photon Excitation Microscopy and Its Applications to Neuroscience. Cell Press50(6): 823-839

Skelin,M., Rupnik, M., Cencic, A. (2010) Pancreatic B-cell lines and their applications in diabetes mellitus research. ALTEX 27: 105-113

Takahashi, K., J. Folmer, and P.A. Coulombe. (1994) Increased expression of keratin 16 causes anomalies in cytoarchitecture and keratinization in transgenic mouse skin. J. Cell Biol. 127:505–520.doi:10.1083/jcb.127.2.505

Toivola, D., Strnad, P., Habtezion, A. and Omary, M. (2010) Intermediate filaments take the heat as stress proteins. Trends in Cell Biology. 20: 79-91.

Toivola, D.M., I. Nakamichi, P. Strnad, S.A. Michie, N. Ghori, M. Harada, K. Zeh, R.G. Oshima, H. Baribault, and M.B. Omary. 2008. Keratin overexpression levels correlate with the extent of spontaneous pancreatic injury. The American journal of pathology. 172:882-892

Weiss, M., Steiner, D.F., Philipson, L.H. (2000) Insulin Biosynthesis, Secretion, Structure, and Structure-Activity Relationships. South Dartmouth (MA):MDText.com, Inc. Available from: https://www.ncbi.nlm.nih.gov/books/NBK279029/ [Updated 2014 Feb 1].

Williams., K, Baucher, H.M., Plenefisch, J. (2015) The Tail Domain Is Essential but the Head Domain Dispensable for C. elegans Intermediate Filament IFA-2 Function. PLoS ONE. 10(3): e0119282. doi: 10.1371/journal.pone.0119282

Wilson, J., and Hunt, T. (2008) Molecular biology of the cell. New York: Garland Science.

Woods, L. C., Berbusse, G. W., & Naylor, K. (2016) Microtubules Are Essential for Mitochondrial Dynamics–Fission, Fusion, and Motility–in Dictyostelium discoideum. Frontiers in Cell and Developmental Biology. 4(19). http://doi.org/10.3389/fcell.2016.00019

Zhong, B., Q. Zhou, D.M. Toivola, G.Z. Tao, E.Z. Resurreccion, and M.B. Omary. (2004) Organspecific stress induces mouse pancreatic keratin overexpression in association with NF-kappaB activation. Journal of cell science. 117:1709-1719.